arXiv:1512.00978v3 [cond-mat.quant-gas] 28 Feb 2016

Coqblin-Schrieffer Model for an Ultra-cold Gas of Ytterbium atoms with Metastable States

Igor Kuzmenko[1], Tetyana Kuzmenko[1], Yshai Avishai[1,2] and Gyu-Boong Jo[3]
[1]*Department of Physics, Ben-Gurion University of the Negev, Beer-Sheva, Israel,*
[2]*NYU-Shanghai, Pudong, Shanghai, China,*
[3]*Department of Physics, The Hong Kong University of Science and Technology, Clear Water Bay, Kowloon, Hong Kong, China*

(Dated: March 1, 2016)

Motivated by the impressive recent advance in manipulating cold ytterbium atoms we explore and substantiate the feasibility of realizing the Coqblin-Schrieffer model in a gas of cold fermionic ^{173}Yb atoms. Making use of different AC polarizabillity of the electronic ground state (electronic configuration $^1S_0$) and the long lived metastable state (electronic configuration $^3P_0$), it is substantiated that the latter can be localized and serve as a magnetic impurity while the former remains itinerant. The exchange mechanism between the itinerant $^1S_0$ and the localized $^3P_0$ atoms is analyzed and shown to be antiferromagnetic. The ensuing SU(6) symmetric Coqblin-Schrieffer Hamiltonian is constructed, and, using the calculated exchange constant J, perturbative renormalization group (RG) analysis yields the Kondo temperature T_K that is experimentally accessible. A number of thermodynamic measurable observables are calculated in the weak coupling regime $T > T_K$ (using perturbative RG analysis) and in the strong coupling regime $T < T_K$ (employing known Bethe ansatz techniques).

PACS numbers: 37.10.Jk, 31.15.vn, 33.15.Kr

I. INTRODUCTION

Ever since its discovery, the physics exposed in cold atom systems proves to be a godsend for elucidating spectacular physical phenomena that are otherwise extremely difficult to access elsewhere[1–21]. Special attention is recently focused on quantum magnetism in general, and impurity problems in particular[22–29]. One of the reasons is that a cold atom system opens a way to study the physical properties of a gas of fermionic atoms with half-integer spin $s \geq \frac{3}{2}$, thereby enabling the study of novel impurity problems. The main goal of this paper is to develop this general idea into an experimental and theoretical framework wherein the Coqblin-Schrieffer model can be realized in an atomic gas of cold ^{173}Yb atoms.

In the "traditional" Kondo effect[30–33], a magnetic impurity of spin $\mathbf{S}$ immersed in a metal host, scatters the itinerant electrons having spin $\mathbf{s}$ ($s = \frac{1}{2}$) through an antiferromagnetic exchange interaction $J\mathbf{s}\cdot\mathbf{S}$ with $J > 0$, and the pertinent dynamics is governed by the s-d exchange Hamiltonian[33]. In the Coqblin-Schrieffer model[33–41], the itinerant fermions and the impurity are both N-fold "spin" degenerate, so that the corresponding Hamiltonian has an SU(N) symmetry. The main difference between the s-d exchange model for spin $S = \frac{1}{2}$ and the Coqblin-Schrieffer model for "spin" $S > \frac{1}{2}$ is that, due to exchange scattering, the change of the z-component of the angular momentum of the impurity is restricted to $0, \pm 1$ in the s-d model, while it is unrestricted in the Coqblin-Schrieffer model. In solid state physics, the high level degeneracy is due to spin-orbit coupling, so that the model is relevant for applications to rare earth impurities. In a gas of ultracold atoms, the degeneracy is due solely to the atomic total angular momentum $\mathbf{F} = \mathbf{I} + \mathbf{J}$, where $\mathbf{I}$ is the nuclear spin and $\mathbf{J}$ is the total (orbital and spin) electronic angular momentum.

Realizing the Coqblin-Schrieffer model in cold fermionic ^{173}Yb atoms is feasible due to a rather unique exchange mechanism. The atoms in the $^1S_0$ ground-state form a Fermi gas with SU(N) symmetry and the atoms in the long-lived $^3P_0$ excited state assume the role of localized magnetic impurities. Both the ground and excited states have spin $F = \frac{5}{2}$ (which is the nuclear spin). The idea is to localize an excited $^3P_0$ atom in a state-dependent optical potential, such that it will serve as a magnetic impurity, immersed in a Fermi gas of ground state $^1S_0$ atoms. The latter is confined in a combination of harmonic and periodic potentials but otherwise are itinerant. We show that an antiferromagnetic exchange interaction exists between the itinerant and localized atoms and that the ensuing exchange scattering is described by the Coqblin-Schrieffer Hamiltonian.

In Sec. II we briefly review the advantage of using degenerate alkaline-earth-like atoms such as Yb and Sr for the study the Kondo effect and its SU(N) extension in cold atom experiments. Then, in Sec. III, we present a general description of the system composed of a mixture of ^{173}Yb atoms in their ground and excited states. Atomic quantum states in the optical potential are described in Subsec. III A, while the exchange interaction between Yb atoms in the ground and excited states is derived in Subsec. III B. This exchange interaction is somewhat unusual because it occurs between the same atoms whose electronic angular momentum is zero. In Subsec. III C we derive the SU(N) Kondo Hamiltonian and estimate the Kondo temperature. Calculations of ob-

servables are detailed in Sec. IV, and naturally divided into the weak and strong coupling regimes. The magnetic susceptibility, entropy and specific heat of the impurity, in the weak coupling regime ($T > T_K$) are estimated in Subsection IV A. Magnetic susceptibility, entropy and specific heat of the impurity in the strong coupling regime ($T < T_K$) are derived in Subsecsection IV B. Our main results are summarized in Sec. V. Details of the derivation of the exchange interaction between two Yb atoms in $^1S_0$ and $^3P_0$ respective atomic states are expanded upon in the Appendix. It is shown and underlined there that precise calculation of the exchange constant requires a detailed knowledge of the atomic wave functions. Although these details are of technical nature, they expose how the exchange interaction determines the scattering length, and demonstrate the extreme sensitivity of the relation between the singlet and triplet scattering lengths on the one hand and the magnitude of the exchange interaction on the other hand. In subsection A 1 we discuss statistics of two atoms and two ions. Electronic wave functions of neutral atoms and positively and negatively charged ions are considered in subsection A 2. Indirect exchange interaction is considered in subsection A 3. It is shown that the exchange is antiferromagnetic. This conclusion does not depend on a chosen model or an approximation but is general property of the second order perturbation theory. Wave function describing motion of interacting atoms is derived in subsection A 4. We derive here expression for the scattering length. In subsection A 5 we compare our results for the scattering length with experimental results of Ref.[52]. In subsection A 6 we express the exchange interaction strength in terms of the scattering lengths. Decay of exchange interaction between atoms due to van der Waals interaction is considered in details in subsection A 7.

II. KONDO EFFECT WITH COLD ALKALINE ATOMS

Recent advance in the techniques of cooling and manipulating degenerate alkaline-earth-like atoms (e.g. ytterbium and/or strontium atoms)[42–44] paves the way for studying novel aspects of interacting Fermi systems. These include non-equilibrium properties such as transport, as well as impurity problems and other facets of quantum magnetism. A key role in these considerations is played by the interplay between the long-lived metastable $^3P_0$ state and the $^1S_0$ ground state, with their enlarged SU(N) spin symmetry for fermionic isotopes[45,46]. Utilizing a narrow singlet-triplet optical transition, for example, alkaline-earth-like atoms have been thought of as a promising candidate for realizing a precise atomic clock[47] or ideal storage of qubits for the application of quantum computing[46].

Here we consider the possible occurrence of the Kondo effect and its SU(N) extensions in a gas of ytterbium atoms. Making use of different AC polarizabilities of the ground-state ($^1S_0$) and the long lived metastable ($^3P_0$) state, the localized $^3P_0$ atoms can serve as magnetic impurities which interact with itinerant ground-state atoms[48–50]. The Kondo effect arises when this interaction is characterized by spin-exchange between $^1S_0$ and $^3P_0$ state. Such spin-exchange interactions has recently been demonstrated[51–53] in fermionic ^{173}Yb atoms.

Realizing the Kondo effect in alkali-earth-like atoms exposes novel aspects of the Kondo physics with SU(N) symmetric interactions that are difficult to elucidate in solid-state based system, because the high SU(N) symmetry arises from the strong decoupling between nuclear and electronic spins in alkali-earth-like atoms. As such, it has attracted much interest in the context of SU(N) Fermi gases both for bulk systems[54–56] and for lattice systems[57]. Here, we focus on the SU(N) Kondo model in the fermionic ^{173}Yb gas, and estimate the Kondo temperature. In cold atom systems, due to the weak magnetic coupling of spin-exchange interactions, the questions still remains whether or not the Kondo temperature is attainable by current experiments. Our finding shows that the Kondo temperature is enhanced by the SU(N) interactions. In electronic systems, this is shown in previous works on heavy fermion systems[33,58] and on carbon nanotube quantum dots[40]. Indeed, the Kondo temperature in cold atom system may also be enhanced by means of the confinement-induced resonance[57] or by the orbital-induced Feshbach resonance[59–62].

III. DESCRIPTION OF THE SYSTEM

Having underlined the peculiar advantage of using alkaline atoms to explore the Kondo effect and its SU(N) extensions, we now focus a cold gas of ^{173}Yb fermionic atoms confined in a shallow harmonic potential. Most of the atoms remain in the ground state $^1S_0$ and form a Fermi sea due to its half integer nuclear spin $I = \frac{5}{2}$ (purple area in Fig. 1). However, a few atoms are found in a long lived excited $^3P_0$ state following a coherent excitation via the clock transition. These excited atoms can be trapped in a state-dependent optical lattice potential as schematically displayed in Fig. 1 (red circles), and can be regarded as localized impurities. The wavelength of the periodic optical potential exceeds the range of interaction between atoms, thereby justifying the assumption that the concentration of excited atoms is small enough so that they are not correlated.

In the following, we describe such mixture of ^{173}Yb atomic system within a model of uncorrelated and localized magnetic impurities. To this end, the details of an exchange interaction between an atom in the ground-state and an atom in an excited state is of crucial importance. Since both atoms in the ground and excited states are in an electronic singlet state, direct exchange interaction between these atoms is absent. There is, however, an indirect exchange, that involves virtual hopping

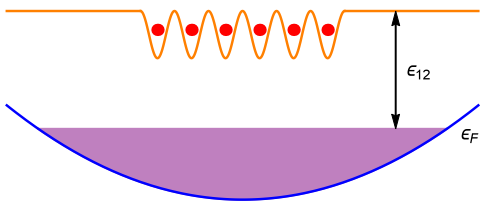

FIG. 1: (color online) Illustration of a "Kondo model" for ^{173}Yb atoms. Atoms in the ground-state $^1S_0$ form a Fermi sea, while atoms in the excited-state $^3P_0$ are trapped in an optical potential and form a dilute concentration of localized magnetic impurities (see details in the text).

of electrons between the atoms such that an atom transforms from the ground state to an excited state, whereas the other atom transforms from an excited state to the ground state. An expression for this exchange interaction is derived below, followed by an analysis of the corresponding impurity problem, that turns out to be a manifestation of the Coqblin-Schrieffer model realized in cold atom systems.

A. Quantum States of ^{173}Yb Atoms with van der Waals Interaction

Before discussing exchange interaction between two Yb atoms it is important to analize the single atom properties because the exchange interaction is crucially dependent on the electronic wave functions of a single atom. An ^{173}Yb atom can be considered as a charged (+2) closed shell rigid ion and two valence electrons. The ground-state $^1S_0$ valence electrons configuration is $6s^2$, while that of the excited state $^3P_0$ is $6s6p$. The excitation energy $\epsilon_{12} = \epsilon_2 - \epsilon_1$ is[63]

$$\epsilon_{12} \;=\; 2.14349 \text{ eV}.$$

The positions of the ion core and the outer electrons are respectively specified by vectors $\mathbf{R}$, $\mathbf{r}_\mathrm{a}$ and $\mathbf{r}_\mathrm{b}$ (Fig. 2).

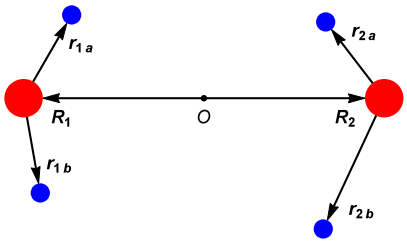

FIG. 2: (color online) Two ytterbium atoms. The position of the rigid ions are $\mathbf{R}_1$ and $\mathbf{R}_2$, positions of the electrons are $\mathbf{r}_{1\mathrm{a}}$, $\mathbf{r}_{1\mathrm{b}}$, $\mathbf{r}_{2\mathrm{a}}$ and $\mathbf{r}_{2\mathrm{b}}$. The origin of the frame is denoted as O.

The ytterbium atoms are trapped by state-dependent trapping potentials $V_{\mathrm{g,x}}(\mathbf{R})$,

$$V_\mathrm{g}(\mathbf{R}) \;=\; V_\mathrm{g}^{(0)} k_\mathrm{g}^2 R^2, \quad R \;=\; |\mathbf{R}|, \tag{1}$$

$$V_\mathrm{x}(\mathbf{R}) \;=\; V_\mathrm{x}^{(0)} \sum_i \sin^2\left(k_\mathrm{x} X_i\right), \tag{2}$$

where i is a Cartesian index. The potential parameters are tuned such that

$$V_\mathrm{g}^{(0)} k_\mathrm{g}^2 \;\ll\; V_\mathrm{x}^{(0)} k_\mathrm{x}^2, \tag{3}$$

and therefore the atoms in the ground state are considered as itinerant atoms, and the atom in the excited state plays a role of the impurity.

In the adiabatic (Born-Oppenheimer) approximation (which is well substantiated in atomic physics), the wave function of a single ytterbium atom is expressed as a product of the wave functions $\Psi(\mathbf{R})$ (for the rigid ion core) and $\psi(\mathbf{r}_a, \mathbf{r}_b)$ (for the valence electrons). The former is considered as a point particle of mass M whose position vector in Cartesian coordinates is $\mathbf{R} = (X, Y, Z)$.

Starting with the core wave functions, recall that the atoms in the ground-state and the excited state are subject to different 3D optical potentials and van der Waals interactions between the atoms. Strictly speaking, we should describe the system by many-particle wave function $\Psi(\mathbf{R}_0; \{\mathbf{R}\}_\mathcal{N})$, where $\mathcal{N}$ is the number of itinerant atoms, $\{\mathbf{R}\}_\mathcal{N} = \{\mathbf{R}_1, \mathbf{R}_2, \ldots, \mathbf{R}_\mathcal{N}\}$, $\mathbf{R}_j$ is the position of an itinerant atom ($j = 1, 2, \ldots, \mathcal{N}$) and $\mathbf{R}_0$ is the position of the impurity atom. When the distance between all the atoms exceeds the range of the vad der Waals interaction, the many-particle wave function splits into a product of single-particle wave functions. When an itinerant atom is placed close to the impurity and all other atoms are far away, the many particle wave function is a product of a two-particle wave function describing interacting pair of atoms, and single particle wave functions describing motion of the other itinerant atoms. Usually, the density of itinerant atoms is low and the probability to find two or more itinerant atoms close to the impurity is negligible small. Therefore, we can describe the many atomic system in terms of two-atomic wave functions. For this purpose we use the notations $\Psi(\mathbf{R}_1, \mathbf{R}_2)$ for the core wave functions pertaining for two atoms in the ground or excited electronic states. They are solutions of the following Schrödinger equation:

$$\mathcal{H}\Psi(\mathbf{R}_1, \mathbf{R}_2) \;=\; \mathcal{E}\Psi(\mathbf{R}_1, \mathbf{R}_2). \tag{4}$$

Here $\mathbf{R}_1$ is the position of the atom in the ground state, $\mathbf{R}_2$ is the position of the atom in the excited state. The two particle Hamiltonian $\mathcal{H}$ is,

$$\mathcal{H} \;=\; \mathcal{H}_\mathrm{g} + \mathcal{H}_\mathrm{x} + W\big(|\mathbf{R}_1 - \mathbf{R}_2|\big). \tag{5}$$

The first or second terms on the right hand side of eq. (5) describe motion of the atom in the groung or excited

state,

$$\mathcal{H}_{\rm g} \;=\; -\frac{\hbar^2}{2M}\,\frac{\partial^2}{\partial \mathbf{R}_1^2} + V_{\rm g}(\mathbf{R}_1), \tag{6}$$

$$\mathcal{H}_{\rm x} \;=\; -\frac{\hbar^2}{2M}\,\frac{\partial^2}{\partial \mathbf{R}_2^2} + V_{\rm x}(\mathbf{R}_2), \tag{7}$$

where M is the atomic mass. Recall that the trapping potentials $V_{\rm g,x}(\mathbf{R})$ are defined in eqs. (1) and (2).

The third term on the right hand side of eq. (5) is the Van der Waals interaction between the ytterbium atoms. Explicitly, it is expressed as,[68]

$$W(R) \;=\; \frac{C_6}{R^6}\left\{\frac{\sigma^6}{R^6} - 1\right\} - \frac{C_8}{R^8}. \tag{8}$$

Here $C_6 = 1.9317\cdot 10^3 E_h a_B^6$, $C_8 = 1.94961\cdot 10^5 E_h a_B^8$ and $\sigma = 9.0109362 a_B$, where $E_h = 27.211$ eV is the Hartree energy and $a_B = 0.52918$ Å is the Bohr radius.

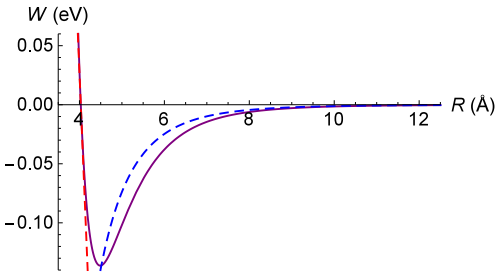

FIG. 3: (color online) Van der Waals interatomic interaction (solid purple curve), its approximation by $-C_6/R^6$ (blue dashed curve) and linear approximation near the classical turning point $R = r_0$ (dashed red line).

Van der Waals potential is illustrated in Fig. 3. It is equal to zero when $R = r_0$, where $r_0 = 4.03122$ Å. At $R = a_0$, the potential $W(R)$ reaches its minimum, $W(a_0) = -0.13428$ eV, where $a_0 = 4.49006$ Å.

1. *Wave Function at Long Distances between the Atoms*

There is a characteristic length λ associated with the van der Waals potential,

$$\lambda \;=\; \left(\frac{MC_6}{\hbar^2}\right)^{1/4} \;=\; 83.1 \text{ Å}. \tag{9}$$

When the distance between the atoms exceeds λ, we can neglect the van der Waals interaction. In this case the two atomic wave function $\Psi(\mathbf{R}_1, \mathbf{R}_2)$ takes the form of a product of two single atomic wave functions, $\Psi_{\rm g}(\mathbf{R}_1)$ and $\Psi_{\rm x}(\mathbf{R}_2)$,

$$\Psi(\mathbf{R}_1, \mathbf{R}_2) \;=\; \Psi_{\rm g}(\mathbf{R}_1)\Psi_{\rm x}(\mathbf{R}_2).$$

The wave functions $\Psi_{\rm g,x}(\mathbf{R})$ are respectively the eigenfunctions of the Hamiltonians $\mathcal{H}_{\rm g}$ and $\mathcal{H}_{\rm x}$, that is,

$$-\frac{\hbar^2}{2M}\,\frac{\partial^2 \Psi_{\rm g,x}(\mathbf{R})}{\partial \mathbf{R}^2} + V_{\rm g,x}(\mathbf{R})\Psi_{\rm g,x}(\mathbf{R}) = \varepsilon \Psi_{\rm g,x}(\mathbf{R}). \tag{10}$$

Consider first the wave function $\Psi_{\rm x}(\mathbf{R})$. When the corresponding energy level $\varepsilon_{\rm imp}$ is deep enough, the wave function of the bound state near the potential minimum at $\mathbf{R} = 0$ can be approximated within the harmonic potential picture as

$$\Psi_{\rm x}(\mathbf{R}) \;=\; \frac{1}{\left(\pi a_{\rm x}^2\right)^{3/4}}\,\exp\left(-\frac{R^2}{2a_{\rm x}^2}\right), \tag{11}$$

where

$$k_{\rm x}a_{\rm x} = \sqrt{\frac{\hbar\omega_{\rm x}}{V_{\rm x}^{(0)}}}, \quad \omega_{\rm x} = \sqrt{\frac{2V_{\rm x}^{(0)}k_{\rm x}^2}{M}}, \quad \varepsilon_{\rm imp} = \frac{3\hbar\omega_{\rm x}}{2}. \tag{12}$$

Next, consider the wave functions $\Psi_{\rm g}(\mathbf{R})$ of the ytterbium atom in the ground state for which the shallow potential wells are not deep enough to form tightly bound states. Hence, we can neglect the "fast" potential relief and take into account just isotropic potential $V_{\rm g}(\mathbf{R})$. Quantum states of atoms in isotropic potential (1) are described by the radial quantum number n [$n = 0, 1, 2, \ldots$], orbital quantum number L [$L = 0, 1, 2, \ldots$] and projection m of the orbital moment on the axis z [$m = -L, -L+1, \ldots, L$]. Due to the centrifugal barrier, only the atoms with $L = 0$ can approach the impurity and be involved in the exchange interaction with it. The wave functions of the states with $L = 0$ found from the Schrödinger equation (10) are,

$$\Psi_{\rm g}^n(\mathbf{R}) = \frac{\mathcal{N}_n}{\sqrt{4\pi}}\,L_n^{(\frac{1}{2})}\left(\frac{\left(R - a_w\right)^2}{a_{\rm g}^2}\right)\exp\left(-\frac{R^2}{2a_{\rm g}^2}\right), \tag{13}$$

where $L_n^{(l+\frac{1}{2})}(\varrho)$ are generalized Laguerre polynomials. The normalization factor is:

$$\mathcal{N}_n \;=\; \left(\frac{2}{\pi a_{\rm g}^6}\right)^{1/4}\sqrt{\frac{2^{n+2}\,n!}{(2n+1)!!}}.$$

The parameters $a_{\rm g}$ and $\omega_{\rm g}$ are defined through,

$$k_{\rm g}a_{\rm g} \;=\; \sqrt{\frac{\hbar\omega_{\rm g}}{V_{\rm g}^{(0)}}}, \qquad \omega_{\rm g} \;=\; \sqrt{\frac{2V_{\rm g}^{(0)}k_{\rm g}^2}{M}}. \tag{14}$$

The corresponding energy levels are

$$\varepsilon_n \;=\; \hbar\omega_{\rm g}\left(2n + \frac{3}{2}\right). \tag{15}$$

The parameter a_w appearing on the right hand side of eq. (13) is a scattering length associated with the van der Waals interaction between the itinerant atom and the localized impurity, see eq. (31) below still without taking exchange into account. It is assumed $a_w \ll a_{\rm g}$. The inequalities (3) imply

$$\omega_{\rm g} \;\ll\; \omega_{\rm x}.$$

Within this framework, the spectrum is nearly continuous and the ytterbium atoms in the ground-state form a Fermi gas. The Fermi energy ϵ_F is such that $\epsilon_F \gg \hbar\omega_{\rm g}$, hence the Fermi gas is 3D.

2. Wave Function at Short Distances between the Atoms

In order to elucidate the behavior of the two atomic wave function within the interval $|\mathbf{R}_1 - \mathbf{R}_2| \lesssim \lambda$, we adopt the semiclassical technique developed in Ref.[67]: Introduce the coordinate $\mathbf{R}_c$ of the center of mass and the relative coordinate $\mathbf{R}$,

$$\mathbf{R}_c \;=\; \frac{1}{2}\,\big(\mathbf{R}_1 + \mathbf{R}_2\big), \qquad \mathbf{R} \;=\; \mathbf{R}_1 - \mathbf{R}_2. \tag{16}$$

In the next step, we employ the following inequalities,

$$k_{\rm g}\lambda \;\ll\; k_{\rm x}\lambda \;\ll\; 1.$$

This enables us to write,

$$V_{\rm x}\Big(\mathbf{R}_c - \frac{\mathbf{R}}{2}\Big) \;=\; V_{\rm x}(\mathbf{R}_c) + O\big(k_{\rm x}\lambda\big).$$

The motion of the atom in the excited state is restricted within the area $|\mathbf{R}_2| \lesssim a_{\rm x}$. Taking into account the inequality $k_{\rm g}a_{\rm x} \ll 1$, we can neglect $V_{\rm g}(R)$ within the intervals,

$$\big|\mathbf{R}_2\big| \;\lesssim\; a_{\rm x}, \qquad \big|\mathbf{R}_1 - \mathbf{R}_2\big| \;\lesssim\; \lambda.$$

Then the two atomic wave function is a product of two functions, $\Psi_c(\mathbf{R}_c)$ and $\Psi_r(\mathbf{R})$, which satisfy the equations,

$$\Big\{ -\frac{\hbar^2}{4M}\,\frac{\partial^2}{\partial \mathbf{R}_c^2} + V_{\rm x}\big(\mathbf{R}_c\big)\Big\}\Psi_c(\mathbf{R}_c) = \mathcal{E}_c\Psi_c(\mathbf{R}_c), \tag{17}$$

$$\Big\{ -\frac{\hbar^2}{M}\,\frac{\partial^2}{\partial \mathbf{R}^2} + W(R)\Big\}\Psi_r(\mathbf{R}) = \mathcal{E}_r\;\Psi_r(\mathbf{R}). \tag{18}$$

Eq. (17) yields the wave function of a bound state near the minimum of $V_{\rm x}(\mathbf{R})$ at $\mathbf{R} = 0$. Before analyzing the wave-function $\Psi_r(\mathbf{R})$, we note that the total energy of the two atom system is

$$\mathcal{E}_n \;=\; \mathcal{E}_c + \mathcal{E}_r.$$

On the other side, this same quantity is also given as:

$$\mathcal{E}_n \;=\; \varepsilon_{\rm imp} + \varepsilon_n,$$

where ε_n is given by eq. (15). For the degenerate Fermi gas, $\varepsilon_n \le \epsilon_F$ and $\varepsilon_{\rm imp} < \epsilon_F$. Usually the Fermi energy ϵ_F is such that the Fermi temperature $T_F = \epsilon_F/k_B$ lies within the interval [see Ref.[51], for example]

$$100\ {\rm nK} \;<\; T_F \;<\; 300\ {\rm nK}.$$

The depth of the van der Waals potential is $W(a_0) = 0.13428$ eV [see Fig. 3]. Then we can neglect $\mathcal{E}_r \sim \varepsilon_n$ with respect to the van der Waals potential (8) at the distances $R \lesssim \lambda$. Then the Schrödinger equation (18) takes the form,

$$\Big\{ -\frac{\hbar^2}{M}\,\frac{\partial^2}{\partial \mathbf{R}^2} + W(R)\Big\}\;\Psi_r\big(\mathbf{R}\big) \;=\; 0. \tag{19}$$

The potential $W(R)$ depends just on the distance R from the impurity. Therefore, the orbital momentum L and its projection m on the axis z are good quantum numbers. Because of the centrifugal barrier, just atoms with $L = 0$ can approach close one to another. Therefore we restrict ourselves by considering just the s-wave (i.e., the wave with $L = 0$). Solution of the equation (19) is evident but rather cumbersome [see Ref.[67] and subsection A 4 for details]. The wave function of the s-wave satisfying eq. (19) is

$$\Psi_n(\mathbf{R}) \;=\; \frac{\psi_n(R)}{\sqrt{4\pi}\;R}, \tag{20}$$

where n is the harmonic quantum number defined by eq. (15). In order to find the radial wave function $\psi_n(R)$, it is useful to employ different approximations in several corresponding intervals as defined below. To this end, we underline the following constraints on the parameters R: r_0, b_0 and λ as follows:

- r_0 is determined from the equation $W(r_0) = 0$. The classical mechanics allows motion of the zero-energy particle in the interval $R > r_0$.

- b_0 is constrained by the inequality,

$$\left|\frac{\sigma^6}{b_0^6} - \frac{C_8}{C_6 b_0^2}\right| \;\ll\; 1.$$

  For $R \ge b_0$, we can approximate $W(R) \approx -C_6/R^6$. Practically, we take $b_0 \approx 10$ Å [see Fig. 3].

- $\lambda = (MC_6/\hbar^2)^{1/4} = 83.1$ Å. In principle, the Wentzel-Kramers-Brillouin (WKB) approximation can be used for for $R \ll \lambda$.

A brief list of approximations per intervals is as follows (see details below): For the interval $r_0 < R \ll \lambda$, we can apply the WKB approximation to solve the Schrödinger equation (18). For the interval $b_0 < R < \lambda$, we can approximate $W(R)$ by $-C_6/R^6$ and solve eq. (18). The interval $R < r_0$ corresponds to classically forbidden region where the wave function decays exponentially. In the following discussions, we find the wave function within each interval. The intervals $r_0 < R \ll \lambda$ and $b_0 < R < \lambda$ overlap one with another since there is a wide interval $b_0 < R \ll \lambda$ where both the WKB approximation and the approximation $W(R) \approx -C_6/R^6$ are valid. Therefore, within this interval both the approaches should give the same solution. We use this condition as as a connection condition for the solutions within two overlapping intervals.

1. Interval $r_0 < R \ll \lambda$: The wave function calculated within the WKB approximation with quantum corrections[67,68] is,

$$\psi_n^{(1)}(R) \;=\; \frac{A_{1n}}{\sqrt{K(R)}}\;\sin\Big(\Phi_r(R) + \frac{\pi}{4}\Big). \tag{21}$$

where

$$\Phi_r(R) \;=\; \int_{r_0}^{R} K(R')dR', \tag{22}$$

$$K(R) \;=\; \frac{1}{\hbar}\,\sqrt{-MW(R)}. \tag{23}$$

When the distance between the atoms exceeds λ, the interaction between the atoms can be neglected and the two-atomic wave function is a product of the single-atomic wave functions (11) and (13). The wave function $\psi_n(R)$ and its derivative $\psi_n'(R)$ are continues at $R=\lambda$. These conditions give

$$A_{1n} \;=\; \frac{2\,\sqrt{k_n\lambda}}{\pi a_{\rm g}}\,\Gamma\!\left(\frac{3}{4}\right)\,\sqrt{1+\left(\frac{a_w-\bar{a}}{\bar{a}}\right)^2}, \tag{24}$$

where

$$k_n \;=\; \frac{2\sqrt{n}}{a_{\rm g}}, \tag{25}$$

the parameters a_w and $\bar{a}$ are given by eqs. (31) and (32) below.

2. Interval $R>b_0$: Within this interval, we can approximate the potential energy by $W(R)\approx -C_6/R^6$. The wave function $\psi_n^{(2)}(R)$ fir this interval is,

$$\psi_n^{(2)}(R) \;=\; A_{2n}\;\tilde{\psi}_{2A}(R)+B_{2n}\;\tilde{\psi}_{2B}(R), \tag{26}$$

where $\tilde{\psi}_{2A}(R)$ and $\tilde{\psi}_{2B}(R)$ are,

$$\tilde{\psi}_{2A}(R) \;=\; \sqrt{\frac{2R}{\lambda}}\;J_{1/4}\!\left(\frac{\lambda^2}{2R^2}\right), \tag{27a}$$

$$\tilde{\psi}_{2B}(R) \;=\; \sqrt{\frac{2R}{\lambda}}\;J_{-1/4}\!\left(\frac{\lambda^2}{2R^2}\right). \tag{27b}$$

There is a large interval $b_0<R\ll\lambda$, where we can approximate $W(R)$ by $-C_6/R^6$ and apply the WKB approximation[67]. Therefore, we can apply the following connection conditions: For any R within the interval $b_0<R\ll\lambda$, the equality $\psi_n^{(1)}(R)=\psi_n^{(2)}(R)$ is valid. This conditions gives,

$$A_{2n} \;=\; -A_{1n}\,\frac{\sqrt{\pi\lambda}}{2}\,\cos\!\left(\Phi_w+\frac{\pi}{8}\right), \tag{28a}$$

$$B_{2n} \;=\; A_{1n}\,\frac{\sqrt{\pi\lambda}}{2}\,\sin\!\left(\Phi_w+\frac{3\pi}{8}\right), \tag{28b}$$

where

$$\Phi_w \;=\; \int_{r_0}^{\infty} K(R)\;dR. \tag{29}$$

The functions $\tilde{\psi}_{2A}(R)$ and $\tilde{\psi}_{2B}(R)$, eq. (27) are shown in Fig. 4, solid lines. It is seen that for $R>\lambda$, the functions $\tilde{\psi}_{2A}(R)$ and $\tilde{\psi}_{2B}(R)$ are well approximated by the linear with R expressions shown by dashed lined. Explicitly, the asymptotic expressions for $\tilde{\psi}_{2A}(R)$ and $\tilde{\psi}_{2B}(R)$ are,

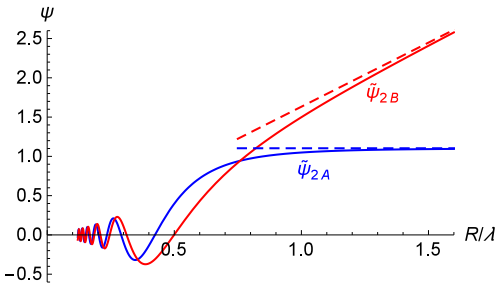

FIG. 4: (color online) Wave functions $\tilde{\psi}_{2A}(R)$ and $\tilde{\psi}_{2B}(R)$, eq. (27) [solid curves] and their asymptotic (30) [dashed lines].

$$\tilde{\psi}_{2A}(R)=\frac{1}{\Gamma(5/4)}\left\{1-\frac{\lambda^4}{20R^4}+O\!\left(\frac{\lambda^8}{R^8}\right)\right\}, \tag{30a}$$

$$\tilde{\psi}_{2B}(R)=\frac{2R/\lambda}{\Gamma(3/4)}\left\{1-\frac{\lambda^4}{12R^4}+O\!\left(\frac{\lambda^8}{R^8}\right)\right\}. \tag{30b}$$

Eqs. (26) and (30) show that the asymptote of the wave function $\psi_n^{(2)}(R)$ at $R\gtrsim\lambda$ is $\psi_n^{(2)}(R)\propto R-a_w$, with the scattering length a_w being[67,68],

$$a_w \;=\; \bar{a}\,\left\{1-\tan\!\left(\Phi_w-\frac{\pi}{8}\right)\right\}, \tag{31}$$

where

$$\bar{a} \;=\; \frac{\lambda}{2^{3/2}}\,\frac{\Gamma\!\left(\frac{3}{4}\right)}{\Gamma\!\left(\frac{5}{4}\right)} \;=\; 39.73\ \text{Å}. \tag{32}$$

For the potential (8), $\Phi_w=226.708$ and

$$a_w \;=\; 34.9\ \text{Å}. \tag{33}$$

B. Exchange Interaction

The angular momentum of the electrons vanishes in the ^{1}S$_0$ and the ^{3}P$_0$ configurations. However, somewhat unexpectedly, when a ytterbium atom in the ground state approaches a localized impurity composed of an excited ytterbium atom such that the distance between them is on the order of the atomic size $R_{\rm A}$, there is an exchange interaction between them. The reason for this exchange interaction is *not* simply due to the direct exchange mechanism that occurs, for example, between two hydrogen atoms. Recall that for the latter, one usually adopts the Heitler-London approximation, designed to avoid the occurrence of two electrons on the same atom. Consequently, the spin part of the Hamiltonian turns out to be proportional to $\mathbf{S}_1\cdot\mathbf{S}_2$, where $\mathbf{S}_{1,2}$ are the electronic spin operators (ore equivalently, the electron contribution

to the atomic spins). But in the case of two ytterbium atoms, each atom is in an s-state, that is, $S_1 = S_2 = 0$. However, while direct exchange interaction is virtually forbidden, there is an indirect exchange as illustrated in Fig. 5: Explicitly, a $6p$ electron tunnels from the atom in the excited state to the atom in the ground state. As a result, we have two ions with parallel electronic orbital moments [Fig. 5(b)]. Then one electron from the $6s$ orbital tunnels from the negatively charged ion to the $6s$ orbital of the positively charged ion. The net outcome is that the atoms "exchange their identity" specified by their electronic quantum states: one atom transforms from the ground state to the excited state, whereas the other atom transforms from the excited state to the ground state. The detailed calculations of the exchange

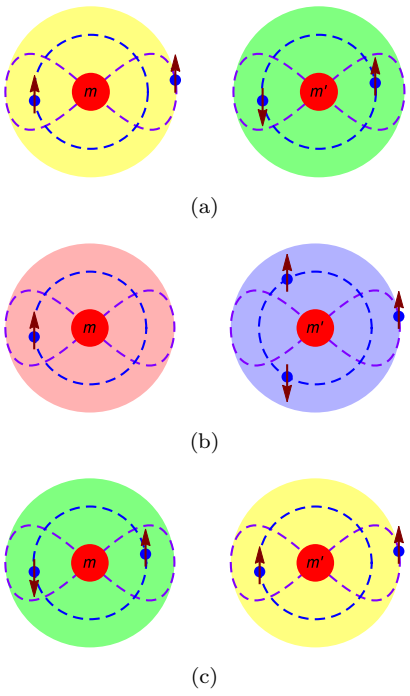

FIG. 5: (color online) Illustration of exchange interaction between ytterbium atoms. Panel (a): Initial quantum state - the first atom (numbered 1) is in the meta-stable state (light yellow disk) and the second one (numbered 2) is in the ground state (light green disk); panel (b): virtual state - the first atom is positively ionized (light red disk), and the second one is negatively charged (light blue disk); panel (c): final state - the first atom is in the ground state and the other one is in the meta-stable state. For all the panels, arrows denote the electronic spin, m or m' is nuclear spin of the first or second atom.

interaction is relegated to the Appendix. Here we describe it rather briefly within the geometry specified in Fig.2. Evaluating the exchange interaction between the ytterbium atoms in the ground and excited states involves two-particle wave function $\Psi_n(\mathbf{R}_0, \mathbf{R}_1)$, where $\mathbf{R}_0$ is the position of the impurity, whereas $\mathbf{R}_1$ and n is the position and quantum numbers of the itinerant atom. For large distance $|\mathbf{R}_1 - \mathbf{R}_0|$ between the atom and the impurity, the two-particle wave function is a product of two wave functions: $\Psi_x(\mathbf{R}_0)$ [Eq. (11)] and $\Psi^n_g(\mathbf{R}_1)$ [Eq. (13)] pertain to the corresponding atoms as being structureless particles in the optical potential (2) and (1). For short distance $|\mathbf{R}_1 - \mathbf{R}_0|$ (where the exchange interaction is nontrivial) we can neglect slow changing harmonic potential (1) and take into account just optical potential (2) and inter-atomic potential (8). The two-particle wave function in this case is a product of two wave functions, one of them describes motion of the center of the mass, and the other one describes relative motion of two atoms. Then the exchange interaction strength is,

$$J_{nn'} = \int d^3\mathbf{R} d^3\mathbf{R}' g\big(|\mathbf{R} - \mathbf{R}'|\big) \Psi^*_n\big(\mathbf{R}, \mathbf{R}'\big) \Psi_{n'}\big(\mathbf{R}, \mathbf{R}'\big),$$

where $\Psi_{n'}\big(\mathbf{R}, \mathbf{R}'\big)$ is a two-particle wave function describing the impurity at $\mathbf{R}$ and the itinerant atom at $\mathbf{R}'$. For short distance $\mathbf{R} - \mathbf{R}'$ between the atoms, the two-atomic wave function can be written as a product of two wave functions, one of them, $\Psi_c(\mathbf{R}_c)$, describes motion of the center of the mass, and the second one, $\Psi_r(\mathbf{R})$, describes relative motion. They satisfy the Schrödinger equations (17) and (18). Integrating over the coordinates of the center of the mass, we get

$$J_{nn'} = \int d^3\mathbf{R}\ g\big(R\big) \Psi^*_n\big(\mathbf{R}\big) \Psi_{n'}\big(\mathbf{R}\big), \qquad (34)$$

where $\Psi_r(\mathbf{R}) \equiv \Psi_n(\mathbf{R})$ is defined in eq. (19).

The exchange interaction between the atom and the impurity separated by the distance R is

$$g(R) = g_0 \zeta(R), \qquad (35)$$

[see subsection A 5 of the Appendix for details]. Here

$$g_0 = 4\pi \int_{r_0}^{\infty} g(R) dR = 1.08879\ \text{eV} \cdot \text{Å}^3, \qquad (36)$$

$$\zeta(R) = \frac{1}{Z} \left(\frac{R}{r_0}\right)^{4\gamma} e^{-\kappa(R - r_0)}, \qquad (37)$$

$$Z = 4\pi \int_{r_0}^{\infty} \left(\frac{R}{r_0}\right)^{4\gamma} e^{-\kappa(R - r_0)}\ R^2 dR = \\ = \frac{4\pi r_0^3 e^{\kappa r_0}}{\big(\kappa r_0\big)^{4\gamma+1}}\ \Gamma\big(4\gamma + 1, \kappa r_0\big), \qquad (38)$$

where $\Gamma(a, b)$ is the incomplete gamma function,

$$\kappa = \kappa_s + \kappa_p = 2.314\ \text{Å}^{-1},$$
$$\gamma = \frac{1 - \beta_s}{\beta_s} + \frac{1 - \beta_p}{\beta_p} = 1.2942.$$

Here $\kappa_{s,p}$ and $\beta_{s,p}$ are parameters of electronic wave functions (A13) and (A14) for $6s$- and $6p$-electrons.

In order to simplify the expression for $J_{nn'}$, we take into account following conditions: The function

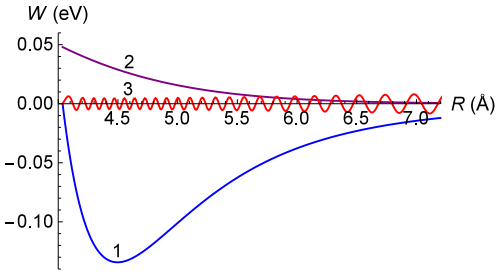

FIG. 6: (color online) Van der Waals interatomic interaction $W(R)$ (curve 1), exchange interaction $10g(R)$ (curve 2) and the wave function $\psi_n^{(1)}(R)$ (curve 3).

$\sin^2(\Phi_k(R)+\pi/4)$ (describing Friedel oscillations) oscillates fast, whereas the functions $g(R)$ and $K(R)$ changes slow (see Fig. 6 for illustration) and therefore can be changed by its averaged value $1/2$. $g(R)$ decreases exponentially and is negligible for $R > b_0$. Therefore we can change the upper limit of integration from b_0 to ∞. Then $J_{nn'}$ takes the form,

$$J_{nn'} = \frac{\sqrt{k_n k_{n'}}}{a_{\rm g}^2}\left\{1+\left(\frac{a_w-\bar{a}}{\bar{a}}\right)^2\right\} G_0, \qquad (39)$$

where

$$G_0 = \frac{8\lambda}{\pi}\,\Gamma^2\!\left(\frac{3}{4}\right)\int\limits_{r_0}^{\infty}\frac{g(R)}{K(R)}\,dR = \\ = 0.02261\ \text{eV}\cdot\text{Å}^3. \qquad (40)$$

When ε_n and $\varepsilon_{n'}$, see eqs. (15) and (25), are near the Fermi energy ϵ_F, then $J = J_{nn'}$ is,

$$J = \frac{\sqrt{2M\epsilon_F}}{\hbar a_{\rm g}^2}\left\{1+\left(\frac{a_w-\bar{a}}{\bar{a}}\right)^2\right\} G_0. \qquad (41)$$

Let us briefly discuss effect of the van der Waals interaction on the exchange coupling. For this purpose we derive expression for $J^{(0)}$ for the absence of the potential $W(R)$ and compare it with eq. (41). When van der Waals potential is absent, the coupling $J^{(0)}_{nn'}$ is,

$$J^{(0)}_{nn'} = \int d^3\mathbf{R}d^3\mathbf{R}'g\big(|\mathbf{R}-\mathbf{R}'|\big)\big|\Psi_{\rm x}(\mathbf{R})\big|^2 \times \\ \times\Psi^n_{\rm g}(\mathbf{R}')\Psi^{n'}_{\rm g}(\mathbf{R}'), \qquad (42)$$

where the wave functions $\Psi_{\rm x}(\mathbf{R})$ and $\Psi^n_{\rm g}(\mathbf{R})$ are given by eqs. (11) and (13).

The function $g(R)$ has maximum at $R = r_0$ and vanishes fast when $R \gg r_0$. The atomic wave functions change slowly within the interval of few r_0, and therefore we can approximate $g(R) \approx g_0\delta(\mathbf{R})$, where g_0 is given by eq. (36). Moreover, the function $\Psi_{\rm x}(\mathbf{R})$ has a maximum at $R = 0$ and vanishes fast when $R \gg a_{\rm x}$. The wave functions $\Psi^n_{\rm g}(\mathbf{R})$ vary slowly on the distance scale of $a_{\rm x}$. Then $|\Psi_{\rm x}(\mathbf{R})|^2$ can be approximated by the δ function. Finally, we get the following estimate of the exchange constant for atoms near the Fermi level: $J^{(0)}_{nn'} = J^{(0)}$, where

$$J^{(0)} = \frac{\sqrt{2M\epsilon_F}}{\hbar a_{\rm g}^2}\,g_0. \qquad (43)$$

Comparing eqs. (41) and (43) shows that van der Waals interaction decreases the exchange coupling as compared with J_0, namely,

$$\frac{J^{(0)}}{J} = \frac{g_0}{G_0}\left[1+\left(\frac{a_w-\bar{a}}{\bar{a}}\right)^2\right]^{-1} = 48.16.$$

Calculations substantiating the decrease of the coupling J due to the van der Waals potential are detailed in subsection A 7 of the Appendix.

C. Kondo Hamiltonian and the Kondo Temperature

Due to centrifugal barrier, only atoms with $L = 0$ interact with the impurity. Omitting the states with nonzero L, we write the Hamiltonian of the system as

$$H = H_0 + H_K, \qquad (44)$$

where

$$H_0 = \sum_{n\mu}\varepsilon_n c^\dagger_{n\mu}c_{n\mu}, \qquad (45)$$

$$H_K = J\sum_{nn'}\sum_{\mu} Z^{\mu\mu}c^\dagger_{n'\mu}c_{n\mu} + \\ + J\sum_{nn'}\sum_{\mu\neq\mu'} X^{\mu\mu'}c^\dagger_{n'\mu'}c_{n\mu}. \qquad (46)$$

Here $c_{n\mu}$ or $c^\dagger_{n\mu}$ is the annihilation or creation operator for atom of Fermi gas with harmonic quantum number n and nuclear spin quantum number $\mu = -\frac{5}{2}, -\frac{3}{2}, \ldots, \frac{5}{2}$. $X^{\mu\mu'} = |\mu\rangle\langle\mu'|$ are the Hubbard operators coupling different degenerate impurity states, and

$$Z^{\mu\mu} = X^{\mu\mu} - \frac{1}{N}\sum_{\mu'}X^{\mu'\mu'}, \qquad N = 6.$$

The density of states for the Hamiltonian H_0 is,

$$\rho(\epsilon) = \sum_n \delta\big(\epsilon-\varepsilon_n\big) = \frac{\Theta(\epsilon)}{2\hbar\omega_{\rm g}}, \qquad (47)$$

where $\Theta(\epsilon)$ is the Heaviside theta function.

Within poor man scaling formalism, the dimensionless coupling $j = J\rho(\epsilon_F)$ satisfies the following scaling equation[33]:

$$\frac{\partial j}{\partial \ln D} = -Nj^2. \qquad (48)$$

Initially, the bandwidth is D_0 and the effective bandwidth D satisfies the inequalities $D_0 \geq D \gg T$. The initial value of $j(D)$, $j(D_0) \equiv j_0$ is,

$$j_0 \;=\; G_0\,\sqrt{\epsilon_F}\,\left(\frac{M}{2\hbar^2}\right)^{\frac{3}{2}}. \tag{49}$$

The scaling equation (48) has the solution,

$$j(T) \;=\; \frac{1}{N\ln\left(T/T_K\right)}, \tag{50}$$

where the Kondo temperature (the scaling invariant of the RG equation) is given by

$$T_K \;=\; D_0\exp\left(-\frac{1}{Nj_0}\right). \tag{51}$$

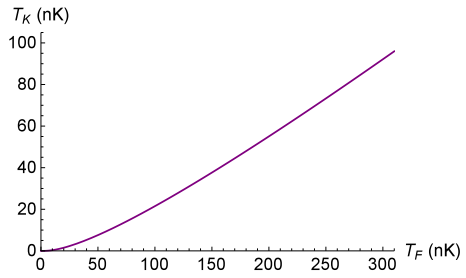

FIG. 7: (color online) Kondo temperature (51) as a function of T_F for $D_0 = T_F/2$.

Kondo temperature (51) as a function of T_F is shown in Fig. 7 for $D_0 = T_F/2$. It is seen that T_K changes in the interval 8 nK$< T_F <$ 92 nK for 50 nK$< T_F <$ 300 nK. For $T_F = 200$ nK, $T_K = 55$ nK.

IV. CALCULATION OF OBSERVABLES

Having set up the model and the corresponding Coqblin-Schrieffer Hamiltonian, it is then possible to predict experimentally measurable observables. At this stage we are content with presenting a few thermodynamics quantities appropriate for a system in thermal equilibrium. These include the impurity contributions to the magnetic susceptibility, specific heat and entropy. Calculations in the weak coupling regime $T > T_K$ require different techniques than those in the strong coupling regime, hence they are presented separately. Specifically, in the weak coupling regime one applies the RG formalism, while in the strong coupling regime the Bethe Ansatz (BA) analyses is employed. Both techniques are well documented and the resulting quantities are universal functions of T/T_K. Since we have already estimated T_K, we can use the known universal expressions for computing and presenting the pertinent thermodynamic quantities.

A. Magnetic Susceptibility, specific heat and entropy in the Weak Coupling Regime

Since the ytterbium atoms are in a quantum state where the total electronic angular momentum is zero, the only contribution to magnetism is due to the nucleus (the nuclear spin is 5/2).

Magnetization: The impurity contribution to the magnetization is defined through the relation[33],

$$\mathbf{M}_{\rm imp} \;=\; g_{\rm Yb}\mu_{\rm n}\Big\{\big\langle\mathbf{S}+\mathbf{s}\big\rangle - \big\langle\mathbf{s}\big\rangle_0\Big\}, \tag{52}$$

where $\langle\cdots\rangle$ indicates thermal averaging with respect to the full Hamiltonian H, whereas $\langle\cdots\rangle_0$ indicates thermal averaging respect to H_0. $g_{\rm Yb} = -0.2592$ is the nuclear g-factor of ^{173}Yb[66], and $\mu_{\rm n}$ is the nuclear magneton,

$$\mu_{\rm n} \;=\; \frac{e\hbar}{2m_{\rm p}c},$$

where $m_{\rm p}$ is the proton rest mass, and c is the speed of light. $\mathbf{S}$ and $\mathbf{s}$ are the nuclear spin operators for the impurity and the itinerant atoms, explicitly written as

$$\mathbf{S} \;=\; \sum_{\mu\mu'}\mathbf{t}_{\mu\mu'}X^{\mu\mu'},$$
$$\mathbf{s} \;=\; \sum_{\mathbf{n}\mathbf{n}'\mu\mu'}\mathbf{t}_{\mu\mu'}c^{\dagger}_{\mathbf{n}\mu}c_{\mathbf{n}'\mu'},$$

where $\hat{\mathbf{t}} = (\hat{t}^x, \hat{t}^y, \hat{t}^z)$ is a vector of the spin 5/2 matrices. In the weak coupling limit, the zero-field magnetic susceptibility calculated within the poor man's scaling technique is[33],

$$\chi(T) \;=\; \frac{\chi_0 T_K}{T}\,\left\{1 - \frac{2}{N\ln\left(T/T_K\right)}\right\}, \tag{53}$$

where

$$\chi_0 \;=\; \frac{g^2_{\rm Yb}\mu^2_{\rm n}}{4T_K}. \tag{54}$$

The quantity $T\chi(T)$ are shown in Fig. 8(a). Within the realm of solid state physics, the mild logarithmic increase of $\chi(T)$ with decreasing temperature in the weak coupling regime of the Coqblin-Schrieffer model, has been discussed experimentally and theoretically a long time ago [see Ref.[33], page 258 Fig.(II)]. It would be of extreme interest to reveal it also within the realm of cold atom physics. For the isolated impurity, $T\chi(T) = T_K\chi_0$ is a constant (Curie law). The fact that $T\chi(T)$ decreases with temperature is a manifestation of the Kondo interaction of the impurity with the Fermi gas. In order to compare the standard SU(2) Kondo model with the SU(N) Coqblin-Schrieffer model, we consider the quantity $X = (T\chi - T_K\chi_0)/(T_K\chi_0)$. For the SU(2) Kondo effect, $X = 1/\ln(T/T_K)$, whereas for the SU(N) Coqblin-Schrieffer model $X = 2/(N\ln(T/T_K))$, i.e., the additional factor $2/N$ appears.

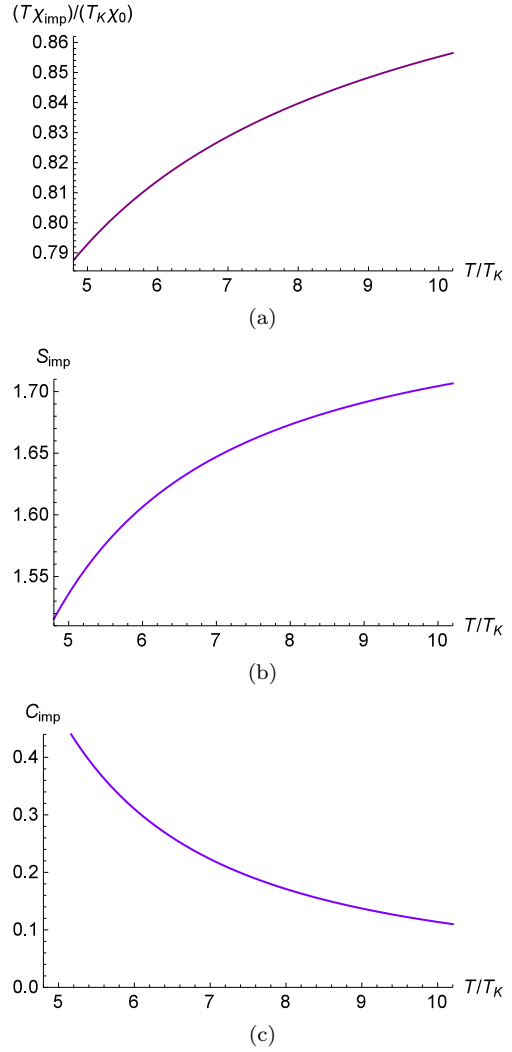

FIG. 8: (color online) $T\chi(T)$ [panel (a)], entropy (56) [panel (b)] and specific heat (57) [panel (c)] as functions of temperature T in the weak coupling regime $T \gg T_K$.

Entropy and specific heat: Calculations of entropy and specific heat start from the free energy of the impurity $F_{\rm imp} = -T\ln(Z/Z_0)$, where Z is the partition function of the entire system and Z_0 is the partition function of the Fermi gas without the impurities,

$$Z = \mathrm{tr}\; e^{-\beta H}, \qquad Z_0 = \mathrm{tr}\; e^{-\beta H_0} \tag{55}$$

The impurity entropy is defined as,

$$S_{\rm imp} = -\frac{\partial F_{\rm imp}}{\partial T}.$$

Poor man's scaling technique which is used in the weak coupling regime $T \gg T_K$ yield the following expression for the impurity contribution to the entropy[33]:

$$S_{\rm imp} \;=\; \ln\left(N\right) - \frac{N^2-1}{N^3}\;\frac{2\pi^2}{3\ln^3(T/T_K)}. \tag{56}$$

The impurity specific heat $C_{\rm imp} = TdS_{\rm imp}/dT$ is,

$$C_{\rm imp} \;=\; \frac{N^2-1}{N^3}\;\frac{2\pi^2}{\ln^4(T/T_K)}. \tag{57}$$

The entropy (56) and the specific heat (57) as functions of temperature are displayed in Figs. 8(b) and 8(c). Kondo effect results in reducing of the entropy with decreasing temperature, whereas $C_{\rm imp}$ increases when temperature decreases. This is the manifestation of the Kondo effect. Note that for the standard SU(2) KE (which is the case $N = 2$), both $S_{\rm imp} - \ln(2)$ and $C_{\rm imp}$ are proportional to the factor 3/8, whereas for the SU(N) Coqblin-Schrieffer model, the factor $(N^2-1)/N^3$ appears.

B. Magnetization, specific heat and entropy in the strong coupling regime

For $T < T_K$, a non-perturbative method should be employed for calculating observables. This is worked out in Ref.[34], where the BA was applied for studying the Coqblin-Schrieffer model at low temperature. Here we apply the formalism derived therein for calculating the pertinent observables in thermal equilibrium. The general structure and behaviour of these quantities is expressed as universal functions of T/T_K. In particular, the magnetic susceptibility $\chi_{\rm imp}$, the ratio $S_{\rm imp}/T$ between the entropy and temperature and the ratio $C_{\rm imp}/T$ between the specific heat and the temperature are characterized by a *finite temperature peak* that becomes more dominant at larger N. This is the main difference between the standard SU(2) Kondo model and SU(N) Coqblin-Schrieffer model: For the SU(2) KE, each one of these three quantities displays a *zero temperature peak*[33,34].

The contribution of the impurity to the free energy at a given magnetic field B (and for $T < T_K$) reads[34],

$$\begin{aligned} F_{\rm imp} \;=\; & -T\sum_{\mu}\int d\epsilon\;\rho_{\rm sc}\left(\epsilon-\mu\Delta_B\right)\ln\left(1+e^{-\epsilon/T}\right) + \\ & +T\int d\epsilon\;\rho_{\rm sc}\left(\epsilon\right)\ln\left(1+e^{-\epsilon/T}\right), \end{aligned} \tag{58}$$

where

$$\Delta_B \;=\; g_{\rm Yb}\mu_n B,$$

the energy ϵ is measured with respect to the Fermi energy. Here $\rho_{\rm sc}(\epsilon)$ is the density of state (DOS) of fermions calculated in the strong coupling limit. At zero temperature, there is a peak in the DOS of width of order T_K near the Fermi energy[33]. This peak is calculated in the framework of slave boson mean field theory[33,40],

$$\rho_{\rm sc}(\epsilon) \;=\; \frac{1}{2}\sum_{\nu=\pm1}\frac{\frac{\pi T_K}{N}}{\left(\epsilon-\nu\epsilon_N\right)^2+\left(\frac{\pi T_K}{N}\right)^2}, \tag{59}$$

where $\epsilon_N = T_K \cos(\pi/N)$. Here we take into account that the electron excitations and hole excitations contribute equally to the free energy[34], and take $g(\epsilon) = g(-\epsilon)$.

Magnetic susceptibility: The zero field impurity magnetic susceptibility $\chi_{\rm imp}$, defined as

$$\chi_{\rm imp} \;=\; -\left(\frac{\partial^2 F_{\rm imp}}{\partial B^2}\right)_{B\to 0},$$

is given by[34],

$$\chi_{\rm imp} \;=\; \frac{\chi_0 T_K}{12T}\; N\left(N^2-1\right)\int \frac{\rho_{\rm sc}(\epsilon)d\epsilon}{\cosh^2\left(\frac{\epsilon}{2T}\right)}, \qquad (60)$$

where χ_0 is given by Eq. (54). The magnetic susceptibility (60) is shown in Fig. 9(a).

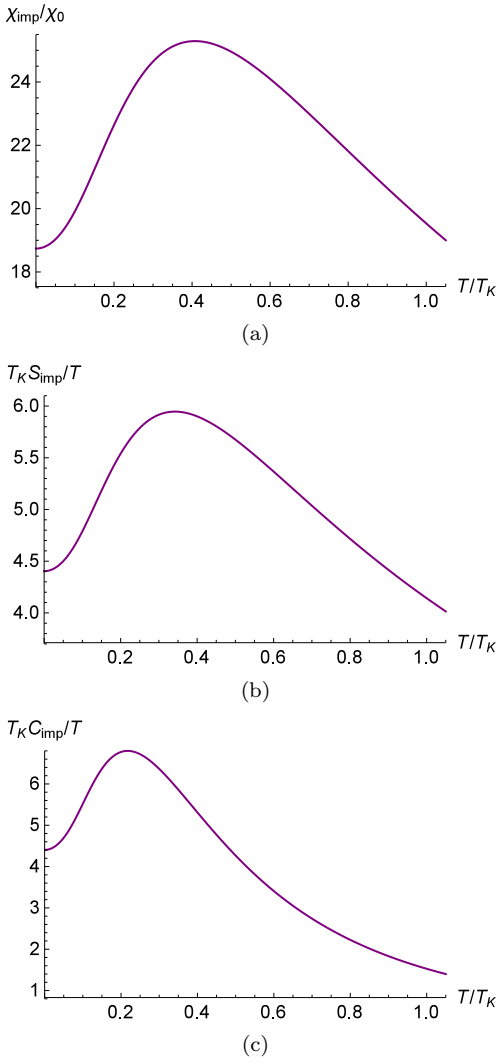

FIG. 9: (color online) Magnetic susceptibility (60) [panel (a)], $S_{\rm imp}/T$ [panel (b)] and $TC_{\rm imp}(T)$ [panel (c)] as functions of temperature in the strong coupling regime $T < T_K$

.

Entropy: Differentiating the free energy (58) and letting the magnetic field $B \to 0$, we obtain an expression for the impurity entropy,

$$S_{\rm imp} \;=\; (N-1)\int d\epsilon\; \rho_{\rm sc}(\epsilon)\ln\left(1+e^{-\epsilon/T}\right) + \\ +\frac{N-1}{T}\int d\epsilon\; \epsilon\rho_{\rm sc}(\epsilon) f(\epsilon), \qquad (61)$$

where $f(\epsilon)$ is the Fermi-Dirac distribution,

$$f(\epsilon) \;=\; \frac{1}{1+e^{\epsilon/T}}.$$

Specific heat: Differentiating the entropy, we get specific heat of the impurity[34],

$$C_{\rm imp} \;=\; \left(N-1\right)\int \left(\frac{\epsilon}{2T}\right)^2 \frac{\rho_{\rm sc}(\epsilon)d\epsilon}{\cosh^2\left(\frac{\epsilon}{2T}\right)}. \qquad (62)$$

The functions $S_{\rm imp}/T$ and $C_{\rm imp}/T$ are shown in Figs. 9(b) and 9(c).

V. CONCLUSIONS

We have studied the feasibility of realizing the Coqblin-Schrieffer model in cold ^{173}Yb atoms. The peculiarities of this framework are as follows: 1) The same atoms are used as itinerant fermions and impurity atom, the only difference is that the former is in an excited state ^{3}P$_0$ and the latter is in the atomic ground-state ^{1}S$_0$. 2) For both ground and excited states, the electronic total angular momentum is zero. 3) Therefore the ensuing exchange interaction is indirect and proceeds through virtual ionic states

$$[(6s^2),(6s6p)] \to [(6s^2 6p)^-,(6s)^+] \to [(6s6p),(6s^2)].$$

The corresponding (positive) exchange energy between the localized and itinerant ytterbium atoms is calculated using reasonable models of atomic wave functions and experimental data for scattering lengths obtained in Ref.[52]. It is then incorporated within a Coqblin-Schrieffer Hamiltonian, and the Kondo temperature is estimated to be $T_K = 0.16 \sim 0.31\ T_F$ for $T_F = 50 \sim 300$ nK. These conditions are favourable for the Kondo effect to be observed in cold fermionic ytterbium laboratories. Using renormalization group analysis, we calculated the magnetic susceptibility, entropy and specific heat of the impurity in the weak coupling regime, $T \gg T_K$. The temperature behaviour of these two quantities is in (qualitative) agreement with calculations carried out in heavy fermion systems, specifically for the Γ_8 quartet $S = \frac{3}{2}$ in a system of Ce impurity immersed in a LaB metal under cubic crystal field[69].

In the second step, we used the machinery of the Bethe Ansatz formalism[70] for the calculation of the impurity contribution to the magnetic susceptibility, entropy and specific heat with the specific parameters pertaining to our Yb system (such as J, T_K, N, $g_{\rm Yb}$ and μ_n). These

results should consist of a reference starting point for relevant experiments.

Acknowledgements
Invaluable correspondence and discussion with Leonid Isaev are highly appreciated. The research of IK, TK and YA is partially supported by the Israel Science Foundation (ISF) under Grant 400/2012. G.B.J acknowledges financial support from the Hong Kong Research Grants Council (Project No.ECS26300014).

Appendix A: Derivation of the Exchange Interaction

In this appendix we derive an expression for the exchange interaction between two atoms of ^{173}Yb. One of them (numbered 1) is the long-lived excited state $^3\mathrm{P}_0$ state with nuclear spin μ, and the other one (numbered 2) is the ground $^1\mathrm{S}_0$ state with nuclear spin μ'. Each atoms is considered as composed of an inert core (charge (+2) closed shell rigid ion) and two valence electrons, as illustrated in Fig. 2. The electron configuration of the excited state $^3\mathrm{P}_0$ is $6s6p$, while that of the ground state is $6s^2$. The positions of the ions are $\mathbf{R}$ and $\mathbf{R}'$.

1. Statistics of Two Atoms and Two Ions

Let us assume that the distance $|\mathbf{R}-\mathbf{R}'|$ between the atomic nuclei is much smaller than a_{x} [the range of localization of the atom in the excited state, see eqs. (11) and (12)]. The optical potentials $V_{\mathrm{g,x}}(\mathbf{R})$, eqs. (1) and (2), are almost constant on this distance scale. Then we can assume that only potential and exchange interactions are active between the atoms. With this assumption, the wave function of two atoms can formally be written as,

$$\big|P_\mu(\mathbf{R}),S_{\mu'}(\mathbf{R}')\big\rangle \;=\; \Psi^\dagger_{\mathrm{x}\mu}(\mathbf{R})\Psi^\dagger_{\mathrm{g}\mu'}(\mathbf{R}')|0\rangle. \quad \text{(A1)}$$

Here $\Psi^\dagger_{\mathrm{x}\mu}(\mathbf{R})$ or $\Psi^\dagger_{\mathrm{g}\mu}(\mathbf{R})$ is a creation operator for the atom in the excited or ground state with nuclear spin μ at position $\mathbf{R}$. A neutral atom of ^{173}Yb has odd number of fermions (70 electrons, 70 protons and 103 neutrons), so that the annihilation and creation operators satisfy anti-commutation relations,

$$\big\{\Psi_{\alpha\mu}(\mathbf{R}),\Psi^\dagger_{\alpha'\mu'}(\mathbf{R}')\big\} \;=\; \delta_{\alpha\alpha'}\delta_{\mu\mu'}\delta(\mathbf{R}-\mathbf{R}'),$$

where $\alpha,\alpha'=\mathrm{g},\mathrm{x}$. Here $\delta_{\alpha\alpha'}$ $[\delta_{\mu\mu'}]$ is the Kronecker delta equal to 1 for $\alpha=\alpha'$ $[\mu=\mu']$ and 0 otherwise, $\delta(\mathbf{R})$ is the Dirac delta function.

The exchange mechanism applicable here is an indirect exchange interaction when an electron virtually tunnels from one atom to another. In order to describe the pertinent exchange interaction, we need to know the wave function of the two ions in the virtual states (middle panel of Fig.2). One of them has charge -1 and electronic configuration $6s^26p$. The other one has charge $+1$ and electronic configuration $6s$. The wave function of the two ions is,

$$\big|E_{\mu m\sigma}(\mathbf{R}),H_{\mu'\sigma'}(\mathbf{R}')\big\rangle \;=\; \Phi^\dagger_{E\mu m\sigma}(\mathbf{R})\Phi^\dagger_{H\mu'\sigma'}(\mathbf{R}')|0\rangle. \quad \text{(A2)}$$

here the index E or H ("electron" or "hole") indicates negatively or positively charged ion. The operator $\Phi^\dagger_{E\mu m\sigma}(\mathbf{R})$ creates a negatively charged ion at position $\mathbf{R}$ with nuclear spin μ, with two electrons at the $6s$ obital and one electron at the $6p$ orbital with a magnetic quantum number m and spin σ. $\Phi^\dagger_{H\mu\sigma}(\mathbf{R})$ creates a positively charged ion at the position $\mathbf{R}$ with nuclear spin μ and one electron with spin σ at the $6s$ orbital. The ions have even number of fermions (71 or 69 electrons, 70 protons and 173 neutrons), therefore the annihilation and creation operators satisfy commutation relations,

$$\begin{aligned}\big[\Phi_{E\mu m\sigma}(\mathbf{R}),\Phi^\dagger_{E\mu' m'\sigma'}(\mathbf{R}')\big] \;&=\\ &=\; \delta_{\mu\mu'}\delta_{mm'}\delta_{\sigma\sigma'}\delta(\mathbf{R}-\mathbf{R}'),\\ \big[\Phi_{H\mu\sigma}(\mathbf{R}),\Phi^\dagger_{H\mu'\sigma'}(\mathbf{R}')\big] \;&=\; \delta_{\mu\mu'}\delta_{\sigma\sigma'}\delta(\mathbf{R}-\mathbf{R}'),\end{aligned}$$

with all other commutators equal to zero.

2. Electronic Wave Functions of Neutral Atoms and Positively and Negatively Charged Ions

In this subsection we present the wave functions of the ground and meta-stable states of the neutral ytterbium atom, as well as the wave functions of the positively and negatively charged ions in their respective virtual states.

a. Wave Functions of Neutral Atom

Ytterbium atom has two electrons outside a closed shell. The configuration of these electrons can be either in $6s^2$ state (ground state), or in the $6s6p$ state (metastable state). The position vectors of the two electrons are denoted as $\mathbf{r}_a$ and $\mathbf{r}_b$. For the ytterbium atom in the ground state, we have

$$\psi_{\mathrm{g}}\big(\mathbf{r}_{\mathrm{a}},\mathbf{r}_{\mathrm{b}}\big) \;=\; \phi_s(\mathbf{r}_{\mathrm{a}})\phi_s(\mathbf{r}_{\mathrm{b}})\chi_S\big(\mathrm{a},\mathrm{b}\big). \quad \text{(A3)}$$

Here $\phi_s(\mathbf{r})$ is the spatial wave function of the $6s$ electron, χ_S is the spin-singlet wave function,

$$\chi_S\big(\mathrm{a},\mathrm{b}\big)=\frac{1}{\sqrt{2}}\Big\{\tilde\chi_\uparrow(\mathrm{a})\tilde\chi_\downarrow(\mathrm{b})-\tilde\chi_\downarrow(\mathrm{a})\tilde\chi_\uparrow(\mathrm{b})\Big\}, \quad \text{(A4)}$$

where $\tilde\chi_\sigma(j)$ is a single-electron spin-σ wave function, $\sigma=\uparrow,\downarrow$ and $j=$a,b. For the ytterbium atom in the metastable state we have,

$$\begin{aligned}\psi_{\mathrm{x}}\big(\mathbf{r}_{\mathrm{a}},\mathbf{r}_{\mathrm{b}}\big) \;=\; \frac{1}{\sqrt{3}}\Big\{&\Phi_1\big(\mathbf{r}_{\mathrm{a}},\mathbf{r}_{\mathrm{b}}\big)\chi_{\bar 1}\big(\mathrm{a},\mathrm{b}\big)-\\ &-\Phi_0\big(\mathbf{r}_{\mathrm{a}},\mathbf{r}_{\mathrm{b}}\big)\chi_0\big(\mathrm{a},\mathrm{b}\big)+\\ &+\Phi_{\bar 1}\big(\mathbf{r}_{\mathrm{a}},\mathbf{r}_{\mathrm{b}}\big)\chi_1\big(\mathrm{a},\mathrm{b}\big)\Big\}. \quad \text{(A5)}\end{aligned}$$

Here $\Phi_m(\mathbf{r}_\mathrm{a},\mathbf{r}_\mathrm{b})$ is the spatial wave function of two electrons in the quantum state $6s6p$ with magnetic quantum number $m=\bar{1},0,1$. Explicitly, they are

$$\Phi_m\big(\mathbf{r}_\mathrm{a},\mathbf{r}_\mathrm{b}\big) \;=\; \frac{1}{\sqrt{2}}\,\Big\{\phi_s\big(\mathbf{r}_\mathrm{a}\big)\phi_m\big(\mathbf{r}_\mathrm{b}\big)-\phi_m\big(\mathbf{r}_\mathrm{a}\big)\phi_s\big(\mathbf{r}_\mathrm{b}\big)\Big\}, \tag{A6}$$

where $\phi_s(\mathbf{r})$ is the spatial wave function of $6s$ electron, $\phi_m(\mathbf{r})$ is the spatial wave function of the $6p$ electron with magnetic quantum number m. The spin-triplet wave functions are χ_μ, where $\mu=\bar{1},0,1$,

$$\begin{aligned}
\chi_1\big(\mathrm{a},\mathrm{b}\big) &= \tilde{\chi}_\uparrow(\mathrm{a})\tilde{\chi}_\uparrow(\mathrm{b}),\\
\chi_{\bar{1}}\big(\mathrm{a},\mathrm{b}\big) &= \tilde{\chi}_\downarrow(\mathrm{a})\tilde{\chi}_\downarrow(\mathrm{b}),\\
\chi_0\big(\mathrm{a},\mathrm{b}\big) &= \frac{1}{\sqrt{2}}\,\Big\{\tilde{\chi}_\uparrow(\mathrm{a})\tilde{\chi}_\downarrow(\mathrm{b})+\tilde{\chi}_\downarrow(\mathrm{a})\tilde{\chi}_\uparrow(\mathrm{b})\Big\}.
\end{aligned} \tag{A7}$$

c. Electronic Densities in the Ground and Excited States

With the electronic wave-functions at hand, we can calculate the corresponding charge densities that is required for the eventual calculations of the exchange interactions. This is carried out in the present subsection. In both cases, the corresponding densities $\rho_g(r)$ and $\rho_x(r)$ depends only on the distance r from the nucleus.

Electronic density for the ground state: For an atom in the ground state $^1\mathrm{S}_0$ with configuration $6s^2$, the density of the $6s$ electrons is given explicitly as,

$$\begin{aligned}
\rho_\mathrm{g}(r) &= 2\int d^3\mathbf{r}'\;\overline{\psi}_\mathrm{g}(\mathbf{r},\mathbf{r}')\psi_\mathrm{g}(\mathbf{r},\mathbf{r}') \;=\\
&= 2\big|\phi_s(r)\big|^2.
\end{aligned} \tag{A10}$$

Here the symbol $\overline{\psi}$ implies complex conjugation of the spatial wave function and Hermitian conjugation of the spin wave function.

b. Wave Function of Positively and Negatively Charged Ions

In the present scheme, the positively charged ion has one electron on the $6s$ orbital. The corresponding wave function is,

$$\psi_{\mathrm{p}\sigma}(\mathbf{r}) \;=\; \phi_s^\mathrm{p}(\mathbf{r})\;\tilde{\chi}_\sigma. \tag{A8}$$

Here $\phi_s^\mathrm{p}(\mathbf{r})$ is the wave function of $6s$ electron. The index p indicates possible "deformation" of the wave function due to the ionization of the atom. The negatively charged ion has two electrons on the $6s$ orbital and one electron on the $6p$ orbital. The corresponding wave function is,

$$\begin{aligned}
\psi_{\mathrm{n}m\sigma}\big(\mathbf{r}_{1\mathrm{a}},\;\mathbf{r}_{1\mathrm{b}},\;\mathbf{r}_{2\mathrm{a}}\big) \;=\; \frac{1}{\sqrt{3}}\,\Big\{&\phi_m^\mathrm{n}\big(\mathbf{r}_{1\mathrm{a}}\big)\phi_s^\mathrm{n}\big(\mathbf{r}_{1\mathrm{b}}\big)\phi_s^\mathrm{n}\big(\mathbf{r}_{2\mathrm{a}}\big)\tilde{\chi}_\sigma(1\mathrm{a})\chi_S\big(1\mathrm{b},2\mathrm{a}\big)+\\
&+\phi_m^\mathrm{n}\big(\mathbf{r}_{1\mathrm{b}}\big)\phi_s^\mathrm{n}\big(\mathbf{r}_{2\mathrm{a}}\big)\phi_s^\mathrm{n}\big(\mathbf{r}_{1\mathrm{a}}\big)\tilde{\chi}_\sigma(1\mathrm{b})\chi_S\big(2\mathrm{a},1\mathrm{a}\big)+\\
&+\phi_m^\mathrm{n}\big(\mathbf{r}_{2\mathrm{a}}\big)\phi_s^\mathrm{n}\big(\mathbf{r}_{1\mathrm{a}}\big)\phi_s^\mathrm{n}\big(\mathbf{r}_{1\mathrm{b}}\big)\tilde{\chi}_\sigma(2\mathrm{a})\chi_S\big(1\mathrm{a},1\mathrm{b}\big)\Big\}.
\end{aligned} \tag{A9}$$

Here $\phi_s^\mathrm{n}(\mathbf{r})$ is the spatial wave function of $6s$ electron, $\phi_m^\mathrm{n}(\mathbf{r})$ is the spatial wave function of the $6p$ electron with magnetic quantum number m. The index n indicates possible deformation of the wave function due to the ionization of the atom. $\chi_S(j,j')$ is the spin-singlet wave function (A4) and $\tilde{\chi}_\sigma(j)$ is a single-electron spin-σ wave function [$\sigma=\uparrow,\downarrow$ and $j,j'=$ 1a,1b,2a].

Electronic density for the excited state: For an atom is in the excited state $^3\mathrm{P}_0$ with configuration $6s6p$, the density of the $6s$ and $6p$ electrons is

$$\rho_\mathrm{x}(r) \;=\; 2\int d^3\mathbf{r}'\;\overline{\psi}_\mathrm{x}(\mathbf{r},\mathbf{r}')\psi_\mathrm{x}(\mathbf{r},\mathbf{r}').$$

Taking into account that the spin wave functions $\chi_m(a,b)$ for different m are orthogonal one to another, we get

$$\rho_\mathrm{x}(r) \;=\; \big|\phi_s(r)\big|^2+\frac{1}{3}\sum_{m=-1}^{1}\big|\phi_m(\mathbf{r})\big|^2.$$

The wave function of electron in the $6p$-state can be written as,

$$\phi_m(\mathbf{r}) \;=\; \sqrt{4\pi}\;\tilde{\phi}_p(r)\;Y_{1m}(\theta,\phi),$$

where $\tilde{\phi}_p(r)$ is a radial function depending just on the distance r from the nucleus and $Y_{1m}(\theta,\phi)$ are spherical harmonics. We chose normalization in such a way that

$$4\pi\int\limits_0^\infty\big|\tilde{\phi}_p(r)\big|^2\;r^2dr \;=\; 1.$$

The spherical harmonics $Y_{lm}(\theta,\phi)$ satisfy the following equality,

$$\sum_{m=-l}^{l}\big|Y_{lm}(\theta,\phi)\big|^2 \;=\; \frac{2l+1}{4\pi}. \tag{A11}$$

Then the density $\rho_{\rm x}(r)$ takes the form,

$$\rho_{\rm x}(r) \;=\; \left|\phi_s(r)\right|^2 + \left|\tilde{\phi}_p(r)\right|^2. \qquad \text{(A12)}$$

d. Asymptotic behavior of the electronic wave functions

When the distance r from the nucleus exceeds the radius of the inner orbitals (which is smaller than the atomic radius), the single electron wave functions $\phi_s(r)$ or the radial wave function $\tilde{\phi}_p(r)$ can be approximated by the following expression,

$$\phi_s(r) = \sqrt{\frac{\mathcal{A}\ \kappa_s^3}{\pi\Gamma\left(\frac{2+\beta_s}{\beta_s}\right)}}\ \left(\kappa_s r\right)^{\frac{1-\beta_s}{\beta_s}}\ e^{-\kappa_s r}, \qquad \text{(A13)}$$

$$\tilde{\phi}_p(r) = \sqrt{\frac{\mathcal{A}\ \kappa_p^3}{\pi\Gamma\left(\frac{2+\beta_p}{\beta_p}\right)}}\ \left(\kappa_p r\right)^{\frac{1-\beta_p}{\beta_p}}\ e^{-\kappa_p r}. \qquad \text{(A14)}$$

Here the parameters κ_ν and β_ν are determined by the ionization energy ε_ν of the atom in the groung $[\nu = s]$ or excited $[\nu = p]$ state,

$$\kappa_\nu = \frac{\sqrt{2m_e\varepsilon_\nu}}{\hbar}, \qquad \beta_\nu = \kappa_\nu a_B,$$

where m_e is the electron mass and a_B is the Bohr's radius. Taking into account the values $\varepsilon_s = 6.2542$ eV and $\varepsilon_p = 4.1107$ eV, we get $\kappa_s = 1.2812$ Å^{-1}, $\kappa_p = 1.0387$ Å^{-1}, $\beta_s = 0.67680$ and $\beta_p = 0.54967$. The dimensionless parameter $\mathcal{A}$ encodes the behavior of the function $\phi_\nu(r)$ inside the atom. In the following, we will consider $\mathcal{A}$ as a fitting parameter.

3. Indirect Exchange Interaction

In the present subsection we consider tunneling of an electron from one atom to another which turns two neutral atoms into two ions or *vice-versa*, two ions into neutral atoms. We consider the cases when both the atoms have the same nuclear spin μ and different spins μ and μ', in turn.

a. The case $\mu = \mu'$

Consider an ^{173}Yb atom in the long-lived excited state ^{3}P$_0$ with nuclear spin μ ($|\mu| \le \frac{5}{2}$). Another ytterbium atom is in the ground ^{1}S$_0$ state with the same nuclear spin μ. The wave function of this state is $|P_\mu(\mathbf{r}), S_\mu(\mathbf{r}')\rangle$, see eq. (A1). The energy of this state is taken to be zero. A quantum transition from a neutral atom to an ion occurs in two cases: when an $6s$ electron tunnels from the atom in the ground state to the atom in the excited state, or when the $6p$ electron tunnels from the atom in the excited state to the atom in the ground state. These quantum transitions can be illustrated as follows:

$$\left|P_\mu(\mathbf{R}), S_\mu(\mathbf{R}')\right\rangle \leftarrow^{6s}\rightarrow \left|E_{\mu m\sigma}(\mathbf{R}), H_{\mu\sigma'}(\mathbf{R}')\right\rangle,$$
$$\left|P_\mu(\mathbf{R}), S_\mu(\mathbf{R}')\right\rangle \leftarrow^{6p}\rightarrow \left|H_{\mu\sigma'}(\mathbf{R}), E_{\mu m\sigma}(\mathbf{R}')\right\rangle.$$

Here the index $6s$ means that the $6s$ electron tunnels from the atom in the ground state (g-atom) to the atom in the excited state (x-atom), whereas the index $6p$ means that the $6p$ electron tunnels from the x-atom to the g-atom. The corresponding tunneling rates are $W_s^{m\sigma\sigma'}$ and $W_p^{m\sigma\sigma'}$. The wave functions of the atoms in the ground and excited states, as well as those of the positively and negatively charged ions are listed in Appendix A 2. Employing these wave functions we can express the hybridization rates $W_s^{m\sigma\sigma'}$ and $W_p^{m\sigma\sigma'}$ in terms of "single-electron" tunneling rates t_s and t_p,

$$W_s^{m\sigma\sigma'}(R) \;=\; \frac{t_s(R)}{2\sqrt{2}}\left\{\delta_{m1}\delta_{\sigma\downarrow}\delta_{\sigma'\downarrow} + \delta_{m\bar{1}}\delta_{\sigma\uparrow}\delta_{\sigma'\uparrow} - \right.$$
$$\left. -\frac{\delta_{m0}}{\sqrt{2}}\left[\delta_{\sigma\uparrow}\delta_{\sigma'\downarrow} + \delta_{\sigma\downarrow}\delta_{\sigma'\uparrow}\right]\right\}, \qquad \text{(A15)}$$

$$W_p^{m\sigma\sigma'}(R) \;=\; -\frac{t_p(R)}{2\sqrt{2}}\left\{\delta_{m1}\delta_{\sigma\downarrow}\delta_{\sigma'\downarrow} + \delta_{m\bar{1}}\delta_{\sigma\uparrow}\delta_{\sigma'\uparrow} - \right.$$
$$\left. -\frac{\delta_{m0}}{\sqrt{2}}\left[\delta_{\sigma\uparrow}\delta_{\sigma'\downarrow} + \delta_{\sigma\downarrow}\delta_{\sigma'\uparrow}\right]\right\}, \qquad \text{(A16)}$$

where $R = |\mathbf{R}_1 - \mathbf{R}_2|$ is the distance between the nuclei,

$$t_s(R) = -\int d^3\mathbf{r}\ \tilde{V}_s(r)\phi_s^*(r)\phi_s(|\mathbf{r} - \mathbf{R}|), \qquad \text{(A17a)}$$

$$t_p(R) = -\int d^3\mathbf{r}\ \tilde{V}_p(r)\tilde{\phi}_p^*(r)\tilde{\phi}_p(|\mathbf{r} - \mathbf{R}|). \qquad \text{(A17b)}$$

Here $\tilde{V}_s(r)$ or $\tilde{V}_p(r)$ is an effective potential of interaction of the $6s$ or $6p$ electron with the other atom,

$$\tilde{V}_s(\mathbf{r}) \;=\; V_{\rm i}(\mathbf{r}) + e^2\int\limits_0^r \rho_{\rm g}(r')\left\{1 + \frac{r'}{r}\right\} r'\ dr',$$

$$\tilde{V}_p(\mathbf{r}) \;=\; V_{\rm i}(\mathbf{r}) + e^2\int\limits_0^r \rho_{\rm x}(r')\left\{1 + \frac{r'}{r}\right\} r'\ dr',$$

where $\rho_{\rm g,x}(r)$ is the electronic density for the ground or excited state, see eqs. (A10) and (A12) in Appendix A 2.

The effective potential $V_s(r)$ or $V_p(r)$ is attractive between an electron of one atom and the rigid core of another atom (partially screened by the outer electrons). When the distance R between the atoms exceeds $R_0 = a_{\rm g} + a_{\rm x}$ (where $a_{\rm g}$ or $a_{\rm x}$ is the atomic radius for the ground or excited state), both $t_s(R)$ and $t_p(R)$ are positive.

It is then reasonable to construct a two-level model Hamiltonian for the low-energy physics of the two atom system. The low-lying two-atomic state is $|P_\mu, S_\mu\rangle$,

whereas the hight-energy two-atomic state is,

$$\big|E_\mu, H_\mu\big\rangle \;=\; \frac{1}{\sqrt{3}}\sum_{m\sigma\sigma'}\Big\{\delta_{m1}\delta_{\sigma\downarrow}\delta_{\sigma'\downarrow}+\delta_{m\bar{1}}\delta_{\sigma\uparrow}\delta_{\sigma'\uparrow}- -\frac{\delta_{m0}}{\sqrt{2}}\Big[\delta_{\sigma\uparrow}\delta_{\sigma'\downarrow}+\delta_{\sigma\downarrow}\delta_{\sigma'\uparrow}\Big]\Big\}\big|E_{\mu m\sigma}, H_{\mu\sigma'}\big\rangle.$$

[The coordinates $\mathbf{R}_{1,2}$ are omitted here for brevity]. The two-level Hamiltonian then reads,

$$\mathcal{H}_{\mu\mu} \;=\; \begin{pmatrix} 0 & \tilde{W}_s-\tilde{W}_p \\ \tilde{W}_s-\tilde{W}_p & \Delta\varepsilon \end{pmatrix}. \qquad \text{(A18)}$$

Here $\tilde{W}_{s,p}$ are,

$$\tilde{W}_\alpha \;=\; \frac{\sqrt{3}}{2\sqrt{2}}\,t_\alpha, \qquad \alpha \;=\; s,\; p. \qquad \text{(A19)}$$

The energy of the ionized state is $\Delta\varepsilon$,

$$\Delta\varepsilon \;=\; \varepsilon_{\rm ion}-\varepsilon_{\rm ea}+\epsilon_1-\epsilon_2 \;=\; 4.4107 \text{ eV},$$

where $\varepsilon_{\rm ion} = 6.2542$ eV is the ionization energy[64] and $\varepsilon_{\rm ea} = -0.3$ eV is the electron affinity[65] of ytterbium. Within second order perturbation theory, neglecting terms of order $\tilde{W}_\alpha^3$ and higher, we get the correction to the energy of the ground state,

$$V_{\mu\mu} \;=\; -\frac{1}{\Delta\varepsilon}\Big\{\tilde{W}_s^2+\tilde{W}_p^2-2\tilde{W}_s\tilde{W}_p\Big\}. \qquad \text{(A20)}$$

b. The case $\mu \neq \mu'$

Now consider an ^{173}Yb atom in the long-lived excited state $^3\mathrm{P}_0$ with nuclear spin μ ($|\mu| \le \frac{5}{2}$). Another ytterbium atom is in the ground $^1\mathrm{S}_0$ state with the same nuclear spin μ. The wave function of this state is $|P_\mu(\mathbf{r}), S_{\mu'}(\mathbf{r}')\rangle$, see eq. (A1). The energy of this state is taken to be zero. Another wave function with the same energy is $|P_{\mu'}(\mathbf{r}), S_\mu(\mathbf{r}')\rangle$.

Quantum transition from the neutral atoms to ions occurs in two cases: when an $6s$ electron tunnels from the atom in the ground state to the atom in the excited state, or when the $6p$ electron tunnels from the atom in the excited state to the atom in the ground state. These quantum transitions can be illustrated as following:

$$\big|P_\mu(\mathbf{R}), S_{\mu'}(\mathbf{R}')\big\rangle \leftarrow^{6s}\rightarrow \big|E_{\mu m\sigma}(\mathbf{R}), H_{\mu'\sigma'}(\mathbf{R}')\big\rangle,$$
$$\big|P_{\mu'}(\mathbf{R}), S_\mu(\mathbf{R}')\big\rangle \leftarrow^{6s}\rightarrow \big|E_{\mu' m\sigma}(\mathbf{R}), H_{\mu\sigma'}(\mathbf{R}')\big\rangle,$$

$$\big|P_\mu(\mathbf{R}), S_{\mu'}(\mathbf{R}')\big\rangle \leftarrow^{6p}\rightarrow \big|H_{\mu\sigma'}(\mathbf{R}), E_{\mu' m\sigma}(\mathbf{R}')\big\rangle,$$
$$\big|P_{\mu'}(\mathbf{R}), S_\mu(\mathbf{R}')\big\rangle \leftarrow^{6p}\rightarrow \big|H_{\mu'\sigma'}(\mathbf{R}), E_{\mu m\sigma}(\mathbf{R}')\big\rangle,$$

where the index $6s$ means that the $6s$ electron tunnels from the atom in the ground state (g-atom) to the atom in the excited state (x-atom), whereas the index $6p$ means that the $6p$ electron tunnels from the x-atom to the g-atom. Corresponding hybridization rates $W_{s,p}^{m\sigma\sigma'}$ are given by eqs. (A15) and (A16).

It is now possible to derive a two-level Hamiltonian similar to that derived in eq. (A18). It should be remembered, however, that in the present case, every level is two-fold degenerate, since the atom in the ground and excited states can have nuclear spin μ or μ'. The 4×4 model Hamiltonian is,

$$\mathcal{H}_{\mu\mu'} \;=\; \begin{pmatrix} \hat{H}_l & \hat{W} \\ \hat{W}^\dagger & \hat{H}_h \end{pmatrix}, \qquad \text{(A21)}$$

where $\hat{H}_{l,h}$ describes the system in the low- or high-energy state,

$$H_\alpha \;=\; \epsilon_\alpha \hat{I}_2, \qquad \alpha = l, h,$$

$\hat{I}_2$ is the 2×2 identity matrix, $\epsilon_l = 0$ and $\epsilon_h = \Delta\varepsilon$. The hybridization term $\hat{W}$ is,

$$\hat{W} \;=\; \begin{pmatrix} \tilde{W}_s & -\tilde{W}_p \\ -\tilde{W}_p & \tilde{W}_s \end{pmatrix}, \qquad \text{(A22)}$$

where $\tilde{W}_{s,p}$ are given by eq. (A19).

Within second-order perturbation theory and neglecting (as before) contributions of order $\tilde{W}^3$ and higher, we get the renormalization of the low-energy levels as,

$$\hat{V}_{\mu\mu'} \;=\; -\frac{1}{\Delta\varepsilon}\,\hat{W}^\dagger\hat{W}.$$

Using eq. (A22), we get

$$\hat{V}_{\mu\mu'} \;=\; -\frac{1}{\Delta\varepsilon}\begin{pmatrix} \tilde{W}_s^2+\tilde{W}_p^2 & -2\tilde{W}_s\tilde{W}_p \\ -2\tilde{W}_s\tilde{W}_p & \tilde{W}_s^2+\tilde{W}_p^2 \end{pmatrix}. \qquad \text{(A23)}$$

Here the diagonal matrix elements describe potential interaction between the atoms without "exchanging" the nuclear spin μ and μ', whereas the nondiagonal matrix elements describe spin-exchange interaction. *It is seen that the exchange is positive that means that it is antiferromagnetic.*

4. Semiclassical Wave Function in Atomic Scattering

Here we solve Schrödinger equation (19) in the framework of semiclassical approximation[67,68]. The potential $W(R)$ depends just on the distance R from the impurity. Therefore, the orbital momentum L and its projection m on the axis z are good quantum numbers. Because of the centrifugal barrier, atoms with nonzero L cannot approach close one to another. Therefore we restrict ourselves by considering just the s-wave (i.e., the wave with $L = 0$). Represent the wave function $\Psi_r(\mathbf{R}) \equiv \Psi_n(\mathbf{R})$ as

$$\Psi_n(\mathbf{R}) \;=\; \frac{\psi_n(R)}{\sqrt{4\pi}\,R}. \qquad \text{(A24)}$$

The radial wave function $\psi_n(R)$ satisfies the 1D Schrödinger equation,

$$\psi_n''(R) + \frac{M}{\hbar^2}\, W(R)\psi_n(R) = 0. \tag{A25}$$

To solve this equation it is useful to employ different approximations in several corresponding intervals as defined below. To this end, we underline the following constraints on the parameters R: r_0, b_0 and λ as follows:

- r_0 is determined from the equation $W(r_0) = 0$. The classical mechanics allows motion of the zero-energy particle in the interval $R > r_0$.
- b_0 is constrained by the inequality,

$$\left|\frac{\sigma^6}{b_0^6} - \frac{C_8}{C_6 b_0^2}\right| \ll 1.$$

  For $R \geq b_0$, we can approximate $W(R) \approx -C_6/R^6$. Practically, we take $b_0 \approx 10$ Å [see Fig. 3].
- $\lambda = (MC_6/\hbar^2)^{1/4} = 83.1$ Å. In principle, the Wentzel-Kramers-Brillouin (WKB) approximation can be used for for $R \ll \lambda$.

A brief list of approximations per intervals is as follows (see details below): For the interval $r_0 < R \ll \lambda$, we can apply the WKB approximation to solve the Schrödinger equation (18). For the interval $b_0 < R < \lambda$, we can approximate $W(R)$ by $-C_6/R^6$ and solve eq. (18). The interval $R < r_0$ corresponds to classically forbidden region where the wave function decays exponentially. In the following discussions, we find the wave function within each interval. The intervals $r_0 < R \ll \lambda$ and $b_0 < R < \lambda$ overlap one with another since there is a wide interval $b_0 < R \ll \lambda$ where both the WKB approximation and the approximation $W(R) \approx -C_6/R^6$ are valid. Therefore, within this interval both the approaches should give the same solution. We use this condition as as a connection condition for the solutions within two overlapping intervals [see eqs. (A31) and (A36) below].

1. Interval $r_0 < R \ll \lambda$: In order to solve equation (18), we apply the WKB approximation with quantum corrections[68]. The wave function within this approximation is,

$$\psi_n^{(1)}(R) \;=\; \frac{A_{1n}}{\sqrt{K(R)}}\, \sin\Big(\Phi_r(R) + \frac{\pi}{4}\Big), \tag{A26}$$

where A_{1n} is unknown constant,

$$\Phi_r(R) \;=\; \int_{r_0}^{R} K(R')dR', \tag{A27}$$

$$K(R) \;=\; \frac{1}{\hbar}\,\sqrt{-MW(R)}. \tag{A28}$$

Here the phase $\pi/4$ takes into account connection of $\psi_n^{(1)}(R)$ with exponentially decaying solution in the classically forbidden interval $R < r_0$ [see Ref.[67,68]].

When $R > b_0$, we can write eq. (A27) as,

$$\Phi_r(R) = \int_{r_0}^{\infty} K(R')\; dR' - \int_{R}^{\infty} K(R')\; dR'. \tag{A29}$$

For any $R \geq b_0$, $K(R)$ can be approximated by $K_0(R)$ given by the equation,

$$K_0(R) \;=\; \frac{\sqrt{MC_6}}{\hbar R^3} \;=\; \frac{\lambda^2}{R^3}.$$

Then the second integral on the right hand side of eq. (A29) can be performed analytically and gives,

$$\int_{R}^{\infty} \frac{\lambda^2\; dR'}{\big(R'\big)^3} \;=\; \frac{\lambda^2}{2R^2}.$$

Taking into account that the first term on the right hand side of eq. (A29) is Φ_w, eq. (29), we can write

$$\Phi_r(R) = \Phi_w - \frac{\lambda^2}{2R^2}. \tag{A30}$$

Then $\psi_n^{(1)}(R)$ for $R > b_0$ takes the form,

$$\psi_n^{(1)}(R) = \frac{A_{1n}R^{3/2}}{\lambda}\; \sin\Big(\Phi_w - \frac{\lambda^2}{2R^2} + \frac{\pi}{4}\Big). \tag{A31}$$

2. Interval $R > b_0$: Within this interval, we can approximate the potential energy by $W(R) \approx -C_6/R^6$ and write the Schrödinger equation (A25) in the form,

$$\lambda^2\; \frac{d^2\psi_n^{(2)}(R)}{dR^2} + \frac{\lambda^6}{R^6}\; \psi_n^{(2)}(R) \;=\; 0, \tag{A32}$$

where λ is given by eq. (9).

General solution of eq. (A32) is,

$$\psi_n^{(2)}(R) \;=\; A_{2n}\; \tilde{\psi}_{2A}(R) + B_{2n}\; \tilde{\psi}_{2B}(R), \tag{A33}$$

where $\tilde{\psi}_{2A}(R)$ and $\tilde{\psi}_{2B}(R)$ are two linearly independent solutions of eq. (A32),

$$\tilde{\psi}_{2A}(R) \;=\; \sqrt{\frac{2R}{\lambda}}\; J_{1/4}\Big(\frac{\lambda^2}{2R^2}\Big), \tag{A34a}$$

$$\tilde{\psi}_{2B}(R) \;=\; \sqrt{\frac{2R}{\lambda}}\; J_{-1/4}\Big(\frac{\lambda^2}{2R^2}\Big), \tag{A34b}$$

A_{2n} and B_{2n} are unknown constants.

When $R \gtrsim \lambda$, the asymptotic expressions for $\tilde{\psi}_{2A}(R)$ and $\tilde{\psi}_{2B}(R)$ are,

$$\tilde{\psi}_{2A}(R) = \frac{1}{\Gamma(5/4)}\; \left\{1 - \frac{\lambda^4}{20R^4} + O\Big(\frac{\lambda^8}{R^8}\Big)\right\}, \tag{A35a}$$

$$\tilde{\psi}_{2B}(R) = \frac{2R/\lambda}{\Gamma(3/4)}\; \left\{1 - \frac{\lambda^4}{12R^4} + O\Big(\frac{\lambda^8}{R^8}\Big)\right\}. \tag{A35b}$$

For $R \ll \lambda$, the asymptotic expressions are,

$$\tilde{\psi}_{2A}(R) = \pi \left(\frac{2R}{\pi\lambda}\right)^{3/2} \sin\left(\frac{\lambda^2}{2R^2} + \frac{\pi}{8}\right), \quad \text{(A36a)}$$

$$\tilde{\psi}_{2B}(R) = \pi \left(\frac{2R}{\pi\lambda}\right)^{3/2} \cos\left(\frac{\lambda^2}{2R^2} - \frac{\pi}{8}\right). \quad \text{(A36b)}$$

The functions $\tilde{\psi}_{2A}(R)$ and $\tilde{\psi}_{2B}(R)$, eq. (A34), and their asymptotes (A35) are shown in Fig. 4, solid and dashed lines. It is seen that for $R > \lambda$, the functions $\tilde{\psi}_{2A}(R)$ and $\tilde{\psi}_{2B}(R)$ are well approximated by their asymptotic expressions[67].

There is a large interval $b_0 < R \ll \lambda$, where we can approximate $W(R)$ by $-C_6/R^6$ and apply the WKB approximation. Therefore, we can apply the following connection conditions: For any R within the interval $b_0 < R \ll \lambda$, the equality $\psi_n^{(1)}(R) = \psi_n^{(2)}(R)$ is valid. This conditions gives,

$$A_{2n} = -A_{1n} \frac{\sqrt{\pi\lambda}}{2} \cos\left(\Phi_w + \frac{\pi}{8}\right), \quad \text{(A37a)}$$

$$B_{2n} = A_{1n} \frac{\sqrt{\pi\lambda}}{2} \sin\left(\Phi_w + \frac{3\pi}{8}\right). \quad \text{(A37b)}$$

Taking into account eqs. (A37) and (A35), we can write the asymptote of the wave function $\psi_n^{(2)}(R)$, eq. (A33), as $\psi_n^{(2)}(R) \propto R - a_w$, with the scattering length a_w given by eq. (31) [see Refs.[67,68]].

3. Interval $R \gtrsim \lambda$: Within this interval, the wave function is given by eq. (13). However, it is convenient to introduce a radial wave function $\psi_{3n}(R)$ similar to eq. (A24),

$$\Psi_{\rm g}^{n00}(\mathbf{R}) = \frac{\psi_n^{(3)}(R)}{\sqrt{4\pi}\, R},$$
$$\psi_n^{(3)}(R) = \frac{2^{3/4}\sqrt{k_n}}{\sqrt{\pi}\, a_{\rm g}} \left(R - a\right), \quad \text{(A38)}$$

where

$$k_n = \frac{2\sqrt{n}}{a_{\rm g}}. \quad \text{(A39)}$$

Here we take into account that $k_n\lambda \ll 1$ and $k_n a \ll 1$, and approximate $\psi_3(R)$ for $R \gtrsim \lambda$ by a linear function.

The wave function $\psi_n(R)$ and its derivative $\psi_n'(R)$ are continues at $R = \lambda$. These conditions give

$$A_{1n} = \frac{2\sqrt{k_n\lambda}}{\pi a_{\rm g}} \Gamma\left(\frac{3}{4}\right) \sqrt{1 + \left(\frac{a_w - \bar{a}}{\bar{a}}\right)^2}. \quad \text{(A40)}$$

5. Comparison of Our Calculations with the Results of Ref.[52]

In Ref.[52], the authors report measurement of scattering lengths for two ytterbium atoms in the "singlet" and "triplet" two particle states [i.e., two particle states with symmetric and antisymmetric spatial wave function]. Explicitly, they are,

$$a_S = (2170 \pm 190)\ \text{Å}, \quad \text{(A41)}$$
$$a_T = (219.5 \pm 2.0)\ \text{Å}. \quad \text{(A42)}$$

In order to compare our results with the measurements of Ref.[52], we consider scattering of ytterbium atoms in the ground state with a localized impurity with taking into account van der Waals and exchange interaction. The van der Waals interaction between the ytterbium atoms is given by eq. (8) [see also Ref.[68]]. The exchange interaction between two atoms separated by distance R is

$$g(R) = \frac{2}{\Delta\varepsilon}\, \tilde{W}_s \tilde{W}_p, \quad \text{(A43)}$$

where $\tilde{W}_{s,p} > 0$ are given by eq. (A19). Recall that positive $g(R)$ means that the corresponding exchange interaction is anti-ferromagnetic.

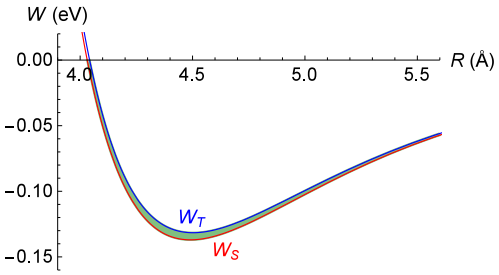

FIG. 10: (color online) $W_S(R)$ and $W_T(R)$, eq. (A46) [red and blue curves]. The green area denotes the exchange interaction strength g_0 [see eq. (A51) below].

The scattering length is given in Ref.[68] in terms of a semiclassical (spin dependent) phase Φ by the following formula,

$$a_\alpha = \bar{a}\left\{1 - \tan\left(\Phi_\alpha - \frac{\pi}{8}\right)\right\}, \quad \text{(A44)}$$

where $\alpha = S$ or T for the two-atomic state with spin wave function which is odd (S) or even (T) under permutation of the atoms, and $\bar{a}$ is given by eq. (32). The semiclassical phase Φ_α is defined as[68] [see eq. (22)],

$$\Phi_\alpha = \frac{\sqrt{M}}{\hbar} \int_{r_\alpha}^{\infty} \sqrt{-W_\alpha(R)}\, dR, \quad \text{(A45)}$$

where

$$W_S(R) = W(R) - g(R),$$
$$W_T(R) = W(R) + g(R). \quad \text{(A46)}$$

r_S or r_T is a classical turning point for zero-energy particle found from the equation $W_S(r_S) = 0$ or $W_T(r_T) = 0$.

For a reference point, we also introduce the scattering length a_w for pure van der Waals potential (without the exchange interaction). Of course, this quantity cannot be experimentally measured,

$$a_w \;=\; \bar{a}\left\{1-\tan\left(\Phi_w-\frac{\pi}{8}\right)\right\}, \qquad \text{(A47)}$$

where $\Phi_w(R)$ is given by eq. (29).
The potentials $W_S(R)$ and $W_T(R)$ are displayed in Fig. 10. It is seen that $W_S(R)$ lies below $W_T(R)$ which is evident due to the antiferromagnetic nature of the exchange interaction.

Realistic van der Waals potential for two ytterbium atoms as given in Eq. (8) is capable of accommodating many two-atomic bound states. This is crucially important because if the potential is such that a new bound-state enters the scattering length jumps from large negative to large positive value. The number N_α of bound states is expressed in terms of the phase Φ_α as[68],

$$N_\alpha \;=\; \left[\frac{\Phi_\alpha}{\pi}-\frac{5}{8}\right]+1, \qquad \text{(A48)}$$

where $[A]$ means the integer part of A. Since $W_S < W_T$ it is expected that $N_S \geq N_T$.

To proceed, we recall the quantities defined in eqs. (36),(37) and (38) and take employ eqs. (A13) and (A14). This enables us to approximate the tunneling rate $t_{s,p}(R)$ [eqs. (A17)] for $R > r_0$ by the following expressions,

$$t_\nu(R)=\frac{\mathcal{A}\kappa_\nu e^2}{\pi\Gamma\left(\frac{2+\beta_\nu}{\beta_\nu}\right)}\left(\kappa_\nu R\right)^{\frac{4(1-\beta_\nu)}{\beta_\nu}}e^{-\kappa_\nu R}. \qquad \text{(A49)}$$

Substituting eqs. (A49) and (A19) into eq. (A43), we get

$$g(R) \;=\; g_0\zeta(R), \qquad \text{(A50)}$$

where $\zeta(R)$ and Z are given by eqs. (37) and (38), with

$$\kappa \;=\; \kappa_s+\kappa_p = 2.314\ \text{Å}^{-1},$$
$$\gamma \;=\; \frac{1-\beta_s}{\beta_s}+\frac{1-\beta_p}{\beta_p} = 1.2942.$$

The value g_0 is

$$g_0 \;=\; \frac{3Z\mathcal{A}^2}{4\pi^2\Gamma\left(\frac{2+\beta_s}{\beta_s}\right)\Gamma\left(\frac{2+\beta_p}{\beta_p}\right)}\,\frac{\kappa_s\kappa_p e^4}{\Delta\varepsilon}\,e^{-\kappa r_0}. \qquad \text{(A51)}$$

To get actual numbers with digital points we need to know the value of $\mathcal{A}$ which contains information on the electronic wave functions of the atoms with due account of electron-electron interactions within the atomic shells. If this interaction is neglected then $\mathcal{A}=1$, but this value yields values of a_S and a_T that are incommensurate with the experimental ones. Exact calculation of $\mathcal{A}$ is beyond the scope of the present work. Therefore, we will be content by tuning $\mathcal{A}$ such that the experimental values of *both* a_S and a_T can be reasonably approximated. This is not at all obvious because there are two quantities and only a single parameter. Moreover, if such fitting requires an unreasonable value of $\mathcal{A}$ then the procedure is meaningless. Note also that the scattering length are extremely sensitive to the strength of the potential. In the present case this procedure proves to be remarkably successful. Taking $\mathcal{A}=0.84095$, we get

$$a_S \;=\; 2173\ \text{Å}, \quad a_T \;=\; 219.1\ \text{Å}, \qquad \text{(A52)}$$
$$a_w \;=\; 34.93\ \text{Å}. \qquad \text{(A53)}$$

These values of a_S and a_T are close to the data given by eqs. (A41) and (A42). This analysis then resolves the subtle problem addressed also in Ref.[71]: How can one get a singlet ground-state and yet $a_S > a_T > 0$? As will be shown below, the reason is that the exchange term deepens the singlet potential and makes $N_S = N_T + 1$.

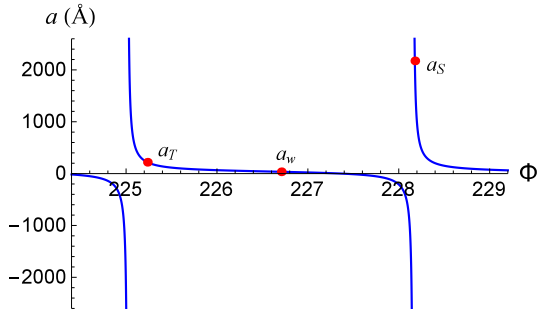

FIG. 11: (color online) Scattering length as a function of the parameter Φ (blue curve). The red points are a_S and a_T, the scattering lengths (A52) for the "singlet" and "triplet" states, as well as a_w, the scattering length (A53) for the pure van der Waals potential. The number of bound states increases by 1 as Φ increases and crossed a singularity. According to the sketch in the figure $N_S = N_T + 1$.

This result underlines the peculiarity of the relation between potential depth and s-wave scattering length (both its magnitude and sign as well as its dependence on the spin-states of the two atoms), as discussed in several papers[72,73]. It is then worthwhile to elaborate further upon it. Usually in the framework of solving the many-body problem for cold-atom systems, the short-range van der Waals potential as well as the exchange interaction are approximated by a delta-function $V(\mathbf{r}) = \frac{4\pi\hbar^2 a}{M}\delta(\mathbf{r})$. Within this approximation, the sign of the scattering length a is commensurate with the nature (repulsive or attractive) of the two-body interaction: $V(\mathbf{r})$ is repulsive (attractive) for $a > 0$ ($a < 0$). If this is the whole story, then the inequality

$$a_S \;>\; a_T \;>\; 0 \qquad \text{(A54)}$$

implies that the "triplet" state energy is lower than the "singlet" state energy that is, the exchange interaction is ferromagnetic. But this conclusion is incommensurate with our results, in which the exchange interaction is

shown to be antiferromagnetic, and yet the inequality (A54) holds. In order to get out of this conundrum, note the following: Eq. (A44) shows that the van der Waals potential can be approximated by the delta-function just when $\Phi_\alpha - \frac{\pi}{8} \ll \frac{\pi}{2}$, i.e., when there is no bound state [Φ_α is constrained to be positive]. However, a realistic van der Waals potential between the Yb atoms can accommodate many bound states[68]. Inspection of Figs. 4 and 6 demonstrates that the wave function strongly oscillates within the range of the van der Waals interaction (recall the relation between bound-states and radial nodes), a property that cannot be obtained from a delta-function potential. The delta-function approximation, while fully justified for treating a dilute gas of weakly interacting atoms should be re-examined for the calculation of exchange interaction that is sensitive to the nature of the fine details of the wave functions. The procedure we used here is to calculate the exchange *ab-initio* using realistic potentials and wave functions and use this exchange interaction for the calculation of the scattering length. The effect of the exchange interaction on the scattering length is illustrated in Fig. 11, upon which we now elaborate. Let us start our analysis by theoretically conceiving a situation where the exchange interaction is absent (of course it cannot be tested experimentally). In this case, the parameter Φ is $\Phi_w = 226.708$ and thus, the singlet and triplet scattering lengths coalesce and equal to a_w given in eq. (A53). When the exchange interaction is switched on (but still remains very weak), we see from Eq. (A46) that the two atom potential $W_S(R)$ in the singlet state is more attractive than the two atom potential $W_T(R)$ in the triplet state. Equivalently, $\Phi_S > \Phi_w > \Phi_T$. Consulting figure 11, we see that as long as $N_S = N_T$ this implies $a_T > a_S$ (in fact a_S can be negative, contrary to experiment). However, at a specific value of the exchange coupling, $g_c = 1.07497$ eV·Å^3, such that $\Phi_S = 72\pi + \frac{5\pi}{8}$, an additional singlet bound state emerges, whereas the number of the triplet bound states remains unchanged. At this value of the exchange coupling, a_S is singular: it tends to $-\infty$ when $g_0 \to g_c^-$, and to $+\infty$ when $g_0 \to g_c^+$ [where g_c^+ or g_c^- means approaching g_c from above or below]. When the exchange interaction strength takes the realistic (calculated) value $g_0 = 1.08879$ eV·Å$^3 > g_c$, then $\Phi_S = 228.177$ and $\Phi_T = 225.235$, and a_S and a_T are given by eq. (A52). Thus, the different number of bound states $N_S = N_T + 1$ implies the inequality (A54) despite the fact that the exchange interaction is *antiferromagnetic*.

6. Derivation of the Exchange Coupling from the Scattering Lengths

In this subsection we discuss derivation of the coupling G_0 of the exchange interaction [see eq. (41)] from the experiment on the scattering length. From a näive point of view, it is tempting to approximate the van der Waals potential and the exchange interaction by delta functions and write the coupling G_0 as,

$$G_0 \;=\; \frac{\hbar^2}{2M}\,\big(a_T - a_S\big).$$

This automatically implies $G_0 < 0$ when $a_S > a_T$, meaning a ferromagnetic exchange coupling. We show here that this procedure is not justified in the present case. In order to derive the coupling G_0 from the experimental value of the scattering lengths, we use eqs. (A44), (A45), (A46) and (A48). From eqs. (A44) and (A48), we get

$$\Phi_\alpha \;=\; \arctan\left(\frac{\bar{a} - a_\alpha}{\bar{a}}\right) + \frac{\pi}{8} + N_\alpha \pi, \qquad \text{(A55)}$$

where $\alpha = S, T$ for the "singlet" and "triplet" states, N_α is the number of bound states. The arctangent function is defined modulo π as,

$$-\,\frac{\pi}{2} \;<\; \arctan\phi \;<\; \frac{\pi}{2}. \qquad \text{(A56)}$$

Then the difference $\Phi_S - \Phi_T$ is,

$$\begin{aligned}\Phi_S - \Phi_T \;&=\; \arctan\left(\frac{\bar{a} - a_S}{\bar{a}}\right) - \\ &-\; \arctan\left(\frac{\bar{a} - a_T}{\bar{a}}\right) + \\ &+\; \pi\big(N_S - N_T\big). \qquad \text{(A57)}\end{aligned}$$

On the other hand, using eq. (A45) we can write this phase difference as

$$\begin{aligned}\Phi_S - \Phi_T \;&=\; \frac{\sqrt{M}}{\hbar}\int\limits_{r_0}^{\infty}\Big\{\sqrt{-W(R) + g(R)} - \\ &-\sqrt{-W(R) - g(R)}\Big\}, \qquad \text{(A58)}\end{aligned}$$

since the differences

$$r_T - r_0 \;\approx\; r_0 - r_S \;\approx\; 0.005 \text{ Å},$$

are negligibly small [see Fig. 10 for illustration], and that allows us to replace r_S and r_T by r_0 as the limits of integration.

In the next step, we employ the estimate $g(R) \ll |W(R)|$ (recall that the attractive part of the van der Waals potential is negative). Expanding the right hand side of eq. (A58) keeping linear terms with $g(R)$ we get,

$$\Phi_S - \Phi_T \;=\; \frac{M}{\hbar^2}\int\limits_{r_0}^{\infty}\frac{g(R)\,dR}{K(R)}, \qquad \text{(A59)}$$

where $K(R)$ is given by eq. (23). Comparing eqs. (A59) and (40) and taking into account eq. (24), we have,

$$G_0 \;=\; \frac{8\hbar^2\lambda}{\pi M}\,\Gamma^2\!\left(\frac{3}{4}\right)\,\Big\{\Phi_S - \Phi_T\Big\}, \qquad \text{(A60)}$$

where the effective range λ of the van der Waals potential is given by eq. (9). Employing eq. (A57) and taking into account that $N_S - N_T = 1$, we express G_0 in terms of the scattering lengths,

$$G_0 = \frac{8\hbar^2\lambda}{M}\,\Gamma^2\left(\frac{3}{4}\right)\left\{1+\frac{1}{\pi}\,\arctan\left(\frac{\bar{a}-a_S}{\bar{a}}\right) - \right.$$
$$\left. - \frac{1}{\pi}\,\arctan\left(\frac{\bar{a}-a_T}{\bar{a}}\right)\right\}. \qquad \text{(A61)}$$

Using the inequalities (A56), one can see that G_0 (A61) is *positive* in spite of the fact that $a_S > a_T$. This is due to the occurrence of an additional "singlet" bound state which leads to the term 1 inside the curly brackets on on the right hand side of eq. (A61).

7. Effect of Potential Scattering on the Exchange Interaction

Let us elaborate on the effect of the van der Waals interaction potential between the atoms on the exchange interaction. As discussed briefly after eq. (41), this is implied by the use of the constant G_0 instead of g_0. Our treatment here is based on the formalism of local density of states (LDOS). The LDOS at short distances between an itinerant atom (^{1}S$_0$) from the impurity (^{3}P$_0$), [that is, $R \lesssim b_0$] is defined as,

$$\rho(\epsilon, R) = \frac{4\pi}{R^2}\sum_{n=0}^{\infty}\left|\psi_n^{(1)}(R)\right|^2\delta(\epsilon-\varepsilon_n), \qquad \text{(A62)}$$

where $\psi_n^{(1)}(R)$ is given by eqs. (21) and (24), and ε_n is given by eq. (15). Employing the fact that the function $\sin^2(\Phi_r(R)+\frac{\pi}{4})$ strongly oscillates, whereas the potential and the exchange interactions change smoothly [see Fig. 6 for illustration], we can approximate $\sin^2(\Phi_r(R)+\frac{\pi}{4})$ by its averaged value $\frac{1}{2}$ and write the "smooth" part of the LDOS as,

$$\rho(\epsilon, R) = \frac{8\lambda}{R^2K(R)}\left\{1+\left(\frac{a_w-\bar{a}}{\bar{a}}\right)^2\right\}\times$$
$$\times\sqrt{\epsilon}\left(\frac{M}{2\hbar^2}\right)^{\frac{3}{2}}\Theta(\epsilon), \qquad \text{(A63)}$$

where we take into account eq. (14) and the equality,

$$a_{\rm g}^2\omega_{\rm g} = \frac{2\hbar}{M}.$$

The exchange interaction between the itinerant atom and the impurity separated a distance R apart is $g(R)$, see eq. (A50). The dimensionless coupling constant j_0 [which is subject to the rescaling analysis] is given by,

$$j_0 = 4\pi\int_{r_0}^{\infty} g(R)\rho(\epsilon_F, R)R^2dR.$$

Using eqs. (A50) and (A63), we get eq. (49). In order to elucidate the effect of the van der Waals interaction on the exchange coupling, we first derive the expression for j_0 *without* potential scattering. In this case, the LDOS near the equilibrium position $R \ll a_{\rm g}$ is,

$$\rho_0(\epsilon) = \sum_n \left|\Psi_{\rm g}^n(0)\right|^2\delta(\epsilon-\varepsilon_n) =$$
$$= \sqrt{\epsilon}\left(\frac{M}{2\hbar^2}\right)^{\frac{3}{2}}\Theta(\epsilon), \qquad \text{(A64)}$$

where the wave function $\Psi_{\rm g}^n(\mathbf{R})$ is given by eq. (13), and ε_n is given by eq. (15). The dimensionless coupling $j_0^{(0)}$ can be defined as,

$$j_0^{(0)} = 4\pi\rho_0(\epsilon_F)\int_{r_0}^{\infty} g(R)R^2dR.$$

Using eqs. (A50) and (A64), we get

$$j_0^{(0)} = g_0\sqrt{\epsilon_F}\left(\frac{M}{2\hbar^2}\right)^{\frac{3}{2}}. \qquad \text{(A65)}$$

Comparing eqs. (A65) and (49) shows that the van der Waals interaction reduces the exchange coupling,

$$\frac{j_0^{(0)}}{j_0} = \frac{g_0}{G_0}\left[1+\left(\frac{a_w-\bar{a}}{\bar{a}}\right)^2\right]^{-1} = 48.16,$$

where g_0 and G_0 are given by eqs. (36) and (40). Thus, $G_0 \ll g_0$, which inevitably leads to a small Kondo temperature. Fortunately, the SU(6) symmetry acts to increase the Kondo temperature, and makes it experimentally attainable.

[1] I. Bloch, J. Dalibard, and W. Zwerger, Rev. Mod. Phys. **80**, 885 (2008).

[2] T. Bourdel, J. Cubizolles, L. Khaykovich, K.M.F. Magalhães, S.J.J.M.F. Kokkelmans, G.V. Shlyapnikov, and C. Salomon, Phys. Rev. Lett. **91**, 020402 (2003).

[3] S.J.J.M.F. Kokkelmans, G.V. Shlyapnikov, C. Salomon, Phys. Rev. **A** 69, 031602 (2004).

[4] C. A. Regal and D. S. Jin, Adv. Atom. Mol. Opt. Phys.

54, 1 (2006).
[5] Q.J. Chen, C.A. Regal, M. Greiner, D.S. Jin, and K. Levin, Phys. Rev. **A** 73, 041601 (2006).
[6] Wenhui Li, G. B. Partridge, Y. A. Liao, and R. G. Hulet, Nuclear Physics **A** 790, 88c (2007).
[7] Wolfgang Ketterle and Martin W. Zwierlein, in "Ultracold Fermi Gases", Proceedings of the International School of Physics "Enrico Fermi", Course CLXIV, Varenna, 20 - 30 June 2006, edited by M. Inguscio, W. Ketterle, and C. Salomon (IOS Press, Amsterdam) 2008.
[8] J. T. Stewart, J. P. Gaebler, and D. S. Jin, Nature **454**, 744 (2008).
[9] W. Li, G. B. Partridge, Y. A. Liao and R. G. Hulet, Int. J. of Mod. Phys. **B** 23, 3195 (2009).
[10] S. Nascimbéne, N. Navon, K. J. Jiang, F. Chevy, and C. Salomon, Nature, **463**, 1057 (2010).
[11] N. Navon, S. Nascimbne, F. Chevy, and C. Salomon, Science **328**, 729, (2010).
[12] Marco Anderlini, Patricia J. Lee, Benjamin L. Brown, Jennifer Sebby-Strabley, William D. Phillips and J. V. Porto, Nature 448, 452 (2007).
[13] S. Trotzky, P. Cheinet, S. Fölling, M. Feld, U. Schnorrberger, A. M. Rey, A. Polkovnikov, E. A. Demler, M. D. Lukin, and I. Bloch, Science 319, 295 (2008).
[14] A. M. Kaufman, B. J. Lester, M. Foss-Feig, M. L. Wall, A. M. Rey, C. A. Regal, arXiv:1507.05586.
[15] Jia Wang, Marko Gacesa, Robin Côté, Phys. Rev. Lett. **114**, 243003 (2015); arXiv:1410.7853.
[16] Russell A. Hart, Pedro M. Duarte, Tsung-Lin Yang, Xinxing Liu, Thereza Paiva, Ehsan Khatami, Richard T. Scalettar, Nandini Trivedi, David A. Huse, Randall G. Hulet, Nature **519**, 211-214 (2015); arXiv:1407.5932.
[17] C.A. Regal, C. Ticknor, J.L. Bohn and D.S. Jin, Nature **424**, 47 (2003).
[18] F. Ferlaino, S. Knoop, M. Berninger, M. Mark, H.-C. Naegerl and R. Grimm, Laser Phys. **20**, 23 (2009); arXiv:0904.0935.
[19] G. Barontini, C. Weber, F. Rabatti, J. Catani, G. Thalhammer, M. Inguscio and F. Minardi, Phys. Rev. Lett. **103**, 043201 (2009).
[20] S. Knoop, F. Ferlaino, M. Mark, M. Berninger, H. Schoebel, H.-C. Naegerl and R. Grimm, Nature Physics 5, 227 (2009).
[21] M. Greiner, Ph.D. thesis, Ludwig Maximilian University of Munich, 2003.
[22] Shintaro Taie, Yosuke Takasu, Seiji Sugawa, Rekishu Yamazaki, Takuya Tsujimoto, Ryo Murakami, and Yoshiro Takahashi, Phys. Rev. Lett. **105**, 190401 (2010).
[23] Yusuke Nishida, arXiv:1508.07098.
[24] Masaya Nakagawa, Norio Kawakami, arXiv:1506.02947.
[25] S. Lal, S. Gopalakrishnan and P. M. Goldbart, arXiv:0910.1579.
[26] L.-M. Duan, E. Demler, and M. D. Lukin, Phys. Rev. Lett. **91**, 090402 (2003).
[27] D. C. McKay and B. DeMarco, Rep. Prog. Phys. **74**, 054401 (2011).
[28] Johannes Bauer, Christophe Salomon and Eugene Demler, Phys. Rev. Lett. **111**, 215304 (2013).
[29] I. Kuzmenko, T. Kuzmenko, Y. Avishai and K. A. Kikoin, Phys. Rev. B**91**, 165131 (2015); arXiv:1402.0187.
[30] J.Kondo, Progr. Theor. Phys. **32**, 37 (1964).
[31] P. Coleman, Physics World **12**, 29 (1995).
[32] P. W. Anderson, Physics World **12**, 37 (1995).
[33] A. C. Hewson, The Kondo Problem to Heavy Fermions (Cambridge University Press, Cambridge, 1993).
[34] V. T. Rajan, Phys. Rev. Lett. **51**, 308 (1983).
[35] P. Schlottmann, Zeitschrift für Physik B: Condensed Matter **51**, 223 (1983).
[36] Andrés Jerez, Natan Andrei, and Gergely Zaránd, Phys. Rev. B **58**, 3814 (1998).
[37] V. Zlatić, B. Horvatić, I. Milat, B. Coqblin, G. Czycholl, and C. Grenzebach, Phys. Rev. B **68**, 104432 (2003); Physica B: Condensed Matter **312-313**, 171 (2002); arXiv:cond-mat/0110179.
[38] V.V. Bazhanov, S.L. Lukyanov, A.M. Tsvelik, Phys. Rev. B **68**, 094427 (2003); arXiv:cond-mat/0305237.
[39] Junya Otsuki, Hiroaki Kusunose, Philipp Werner and Yoshio Kuramoto, J. Phys. Soc. Jpn. **76**, 114707 (2007); arXiv:0708.0718.
[40] Igor Kuzmenko, Yshai Avishai, Phys. Rev. B**89**, 195110 (2014); arXiv:1310.6563.
[41] H.-U. Desgranges, Physica B: Condensed Matter, **454**, 135 (2014); arXiv:1309.3749.
[42] Takeshi Fukuhara, Yosuke Takasu, Mitsutaka Kumakura, and Yoshiro Takahashi, Phys. Rev. Lett. **98**, 030401 (2007).
[43] Y.N.Martinez de Escobar, P.G. Mickelson, M. Yan, B.J. DeSalvo, S.B. Nagel, and T.C. Killian, Phys. Rev. Lett. **103**, 200402 (2009).
[44] S. Stellmer, R. Grimm, and F. Schreck, Physical Review A **84**, 043611 (2011).
[45] A.J.Daley Quantum Information Processing **10**, 865 (2011).
[46] Miguel A.Cazalilla and Ana Maria Rey, Reports on Progress in Physics **77**, 124401 (2014).
[47] Andrei Derevianko and Hidetoshi Katori, Reviews of Modern Physics **83**, 331 (2011).
[48] A. V. Gorshkov, M. Hermele, V. Gurarie, C. Xu, P. S. Julienne, J. Ye, P. Zoller, E. Demler, M. D. Lukin, and A. M. Rey, Nature Physics **6**, 289 (2010).
[49] Michael Foss-Feig, Michael Hermele and Ana Maria Rey, Physical Review A **81** 051603 (2010).
[50] Kaden R. A. Hazzard, Victor Gurarie, Michael Hermele, and Ana Maria Rey, Physical Review A **85** 041604 (2012).
[51] G. Cappellini, M. Mancini, G. Pagano, P. Lombardi, L. Livi, M. Siciliani de Cumis, P. Cancio, M. Pizzocaro, D. Calonico, F. Levi, C. Sias, J. Catani, M. Inguscio, and L. Fallani Phys. Rev. Lett. **113**, 120402 (2014).
[52] F. Scazza, C. Hofrichter, M. Fofer, P. C. De Groot, I. Bloch, and S. Folling, Nature Physics **10**, 779 (2014); *ibid*: correction notice, (2015).
[53] X. Zhang, M. Bishof, S. L. Bromley, C. V. Kraus, M. S. Safronova, P. Zoller, A. M. Rey, and J. Ye, Science **345**, 1467 (2014).
[54] S. K. Yip, B.-L. Huang and J.-S. Kao, Phys. Rev. A **89**, 043610 (2014); arXiv:1312.6765. .
[55] M. A. Cazalilla, A. F. Ho, and M. Ueda, New Journal of Physics, **11**, 103033 (2009).
[56] G. Pagano, M. Mancini, G. Cappellini, P. Lombardi, F. Schafer, H. Hu, X.-J. Liu, J. Catani, C. Sias, M. In- guscio, and L. Fallani, Nature Physics **10**, 198 (2014).
[57] R. Zhang, D. Zhang, Y. Cheng, W. Chen, P. Zhang, and H. Zhai, arXiv:1509.01350 (2015).
[58] C. Pepin, P. Coleman, arXiv:cond-mat/0211284. ; P. Coleman, Lectures on the Physics of Highly Correlated Electron Systems VI, Editor F. Mancini, American Institute of Physics, New York (2002), p 79 - 160.
[59] R. Zhang, Y. Cheng, H. Zhai, and P. Zhang, Phys. Rev.

Lett. **115**, 135301 (2015).
[60] G. Pagano, M. Mancini, G. Cappellini, L. Livi, C. Sias, J. Catani, M. Inguscio, and L. Fallani, arXiv:1509.04256 (2015).
[61] M. Hofer, L. Riegger, F. Scazza, C. Hofrichter, D. R. Fernandes, M. M. Parish, J. Levinsen, I. Bloch, and S. Folling, arXiv:1509.04257 (2015).
[62] Yusuke Nishida, Phys. Rev. Lett. 111, 135301 (2013).
[63] W. F. Meggers and J. L. Tech, J. Res. Natl. Bur. Stand. (U.S.) **83**, 13 (1978).
[64] W. F. Meggers and J. L. Tech, J. Res. Natl. Bur. Stand. (U.S.) **83**, 13 (1978).
[65] T. Andersen, "Atomic negative ions: Structure, dynamics and collisions". Physics Reports **394**, 157 (2004).
[66] Masses, nuclear spins, and magnetic moments: I. Mills, T. Cvitas, K. Homann, N. Kallay, and K. Kuchitsu, in Quantities, Units and Symbols in Physical Chemistry, Blackwell Scientific Publications, Oxford, UK, 1988.
[67] G. F. Gribakin and V. V. Flambaum, Phys. Rev. A **48**, 546 (1993).
[68] Masaaki Kitagawa, Katsunari Enomoto, Kentaro Kasa, Yoshiro Takahashi, Roman Ciuryło, Pascal Naidon, and Paul S. Julienne, Phys. Rev. A **77**, 012719 (2008); arXiv:0708.0752.
[69] P. Schlottmann, Solid State Commun. **57**, 73 (1986).
[70] A. M. Tsvelik and P. B. Wiegman, J. Phys. C **15**, 1707 (1982); N. Andrei, K. Furuya and J. H. Lowenstein, Rev. Mod. Phys. **55** 331 (1983).
[71] L. Isaev and A. M. Rey, Phys. Rev. Lett. **115**, 165302 (2015).
[72] Cheng Chin, Rudolph Grimm, Paul Julienne and Eite Tiesinga, Rev. Mod. Phys. **82**, 1225 (2010).
[73] Caroline L. Blackley, Paul S. Julienne, and Jeremy M. Hutson, Phys. Rev. **A** 89, 042701 (2014).